Study of RF and Neutral Beam Heating of Large Tokamaks

J.E. Scharer, R.W. Conn, and D.T. Blackfield

December 1975

UWFDM-148

FUSION TECHNOLOGY INSTITUTE

UNIVERSITY OF WISCONSIN

MADISON WISCONSIN

Study of RF and Neutral Beam Heating of Large Tokamaks

J.E. Scharer, R.W. Conn, and D.T. Blackfield

Fusion Technology Institute
University of Wisconsin
1500 Engineering Drive
Madison, WI 53706

http://fti.neep.wisc.edu

December 1975

UWFDM-148

Study of Radiofrequency and Neutral Beam Heating of Large Tokamaks

J. E. Scharer*, R. W. Conn and D. T. Blackfield

December 1975

UWFDM-148

Fusion Technology Program
Nuclear Engineering Department
University of Wisconsin
Madison, Wisconsin 53706

*Department of Electrical and Computer Engineering

Legal Notice

"This report was prepared by the University of Wisconsin as an account of work sponsored by the Electric Power Research Institute, Inc. ("EPRI"). Neither EPRI, members of EPRI, nor the University of Wisconsin, nor any person acting on behalf of either:

"a. Makes any warranty or representation, express or implied, with respect to the accuracy, completeness, or usefulness of the information, apparatus, method, or process disclosed in this report may not infringe privately owned rights; or

"b. Assumes any liabilities with respect to the use of, or for damages resulting from the use of, any information, apparatus, method of process disclosed in this report."

TABLE OF CONTENTS

Abstract

We present studies of wave and neutral beam heating of tokamak plasma. The leading wave heating candidates include low frequency Alfvén waves, fast magnetosonic waves, lower hybrid waves, and electron cyclotron waves and these are briefly surveyed. A more detailed consideration is given to the fast magnetosonic wave and its use in heating a tokamak reactor to ignition. A conceptual magnetosonic wave launching system compatible with reactor plasmas is also described. The status of neutral beam heating, the requirements on injection energies, and the resulting heating profiles for reactor plasmas are described. Finally a comparison of RF (radiofrequency) and neutral beam heating is presented. Neutral beams enjoy a very good agreement between present theory and experiment. However, potential penetration and heating of the plasma core and the required source development for reactors favor RF heating. The advantages and problems associated with extrapolating both techniques to reactor plasmas are described. It is concluded that a high priority should be given to definitive high power RF tokamak heating experiments to clarify the physics base. A large effort on high energy neutral beam source development as is currently underway is also required.

1. Introduction

It is clear that a supplementary heating system will be required to heat tokamak plasmas from the ohmic heating limit of a few keV to the tens of keV required for a power producing reactor. As the limits of efficient ohmic heating are reached, supplementary heating will begin to occupy the center stage in the overall fusion program. At present, the two main supplemental heating methods are RF heating and neutral beam injection. These two schemes differ in a fundamental way because wave heating depends on collisionless wave-particle interactions while neutral beam heating is based on particle-particle collisions.

Historically, waves in plasmas have played a very basic role. Since there is a wide range of frequencies and wave types available, there are a variety of absorption mechanisms which can be used to heat plasmas. In general, low power wave-plasma experiments are in good agreement with theory. High power wave-plasma experiments, on the other hand, are less clearly explained.
It is the sensitivity of the heating mechanism to wave frequency and to wave type which gives RF heating some of its attractive advantages. These include the ability to selectively heat one of the plasma species, and the good potential for wave penetration. Thus it may be feasible to use RF to adjust the spatial heating profile. Further, the status of high power RF sources up to the level of 5 MW is quite well developed at efficiencies of 50-70%. Thus, what is needed is a much more vigorous program to provide definitive tests of the viability of high power RF heating and the efficiency of coupling the source energy to the plasma.

In this report we discuss the leading alternatives for RF heating, develop a detailed concept for fast magnetosonic wave heating of a reactor plasma and discuss the requirements for the launching structure. We then review the status of neutral beam heating and the requirements and properties for a reactor heating system. Finally, we present a qualitative comparison of RF and neutral beam heating schemes listing both their advantages and their remaining problems.

2. Potential Wave Heating Modes

There are a number of wave heating modes which have a potential for heating tokamak plasmas. The most promising are (1) fast magnetosonic wave heating, $\omega = 2\omega_{cD}$ (ω_{cD} is the deuteron ion cyclotron frequency) or the two-ion hybrid frequency, $\omega = \omega_{2IHR} \sim (\omega_{cD}\ \omega_{cT})^{1/2}$ for 50% D/50% T plasmas, (2) lower hybrid wave heating, $\omega \sim \omega_{LH} \sim \omega_{pi}$, (3) low frequency Alfvén modes, $\omega << \omega_{cD}$, and (4) electron cyclotron modes, $\omega \sim \omega_{ce}$. In all cases, the wave must be generated at high power levels ~1-100 MW for plasmas of fusion interest, it must be able to penetrate to the plasma core and be absorbed there, and it must have a sufficiently high Q in the toroidal cavity so that plasma absorption dominates the wall losses.

The frequency of these waves ranges from low frequency Alfvén waves (f ~ 1 MHz) to the fast magnetosonic waves (f ~ 60 MHz) to the lower hybrid mode (f ~ 2 GHz) to electron cyclotron waves (f ~ 100 GHz). Present day technology shows that the power and efficiency of generators drops from ~10 MW @ 70% for 1 MHz to 5 MW @ 60% for 60 MHz to 200 KW @~50% for 800 MHz to 1 kW @ ~30-50% for 80 GHz. However, development programs promise to produce 10 MW tetrode modules @ 60 MHz, 1 MW klystrons @ 2 GHz, and 100 kW gyrotrons @ 100 GHz. ($1\ GHz = 10^3\ MHz = 10^9\ Hz$).

Thus, wave sources exist with good efficiencies so that supplementary heating that is equal to or greater than present day ohmic heating can be contemplated. The method of launching this wave energy into a large torus differs with wave type. Waveguide arrays of convenient size are utilized to launch electron cyclotron and lower hybrid modes. Waveguide or coil launching of fast magnetosonic waves is envisioned. Experiments conducted on the ST tokamak with coils have provided good coupling of the magnetosonic wave.[1,2,3,4] Only low power experiments have been conducted with low frequency Alfvén waves but a coil structure located in the wall is envisioned to provide coupling.

Ion cyclotron heating has been used in the early B-65 and in the Model C Stellarator experiments at megawatt power levels. Overall ion temperature increases of 600 eV and local ion temperature increases in a mirror region of 2000 eV were observed in the C-Stellarator.[5,6] In these smaller plasma diameter experiments, the slow or shear magnetosonic wave was excited. For larger tokamaks the fast or compressional magnetosonic mode is more easily excited. The launching structure together with the plasma properties determine the absorption of the fast magnetosonic wave. The theory for these modes was first examined by Adam and Samain.[7] Ivanov, Kovan, and Los'[8] first observed the fast-wave toroidal eigenmodes. Perkins[9] theoretically analyzed these eigenmodes and the detailed experimental verification of the eigenmode resonances and absorption processes were performed on the ST tokamak.[3] In these experiments, there was a significant production of impurities. This has been attributed to the low field and low current required to obtain a resonance for the ST tokamak and the heating of particles on ion banana orbits that intercept the wall.[10] It is expected that these problems will be alleviated in larger tokamaks for

which the wave heating system is designed to heat the plasma core. Fast magnetosonic wave experiments are currently being carried out on the French TFR tokamak. The propagation and absorption of the fast magnetosonic wave ($\omega \approx 2\omega_{ci} \approx k_{\perp} v_A$) is considered in detail in section 3.

In the lower hybrid wave heating approach an electromagnetic wave is launched by means of waveguide feeds. The wave propagates nearly perpendicular to the toroidal magnetic field and moves up the plasma density gradient. It also exhibits a wave resonance where the fields become very large at the density corresponding to the lower hybrid frequency. For most plasmas the lower hybrid frequency occurs well below the electron cyclotron frequency but well above the ion cyclotron frequency. This frequency is given by

$$\omega_{LH}^2 = \omega_{pi}^2 \, \omega_{ce} \, \omega_{ci} / (\omega_{pi}^2 + \omega_{ce} \, \omega_{ci}) \qquad (1)$$

which for tokamak plasmas ($\omega_{pi}^2 \lesssim \omega_{ce}\omega_{ci}$) is approximately the ion plasma frequency $\omega_{LH} \simeq \omega_{pi}$.

A most important condition on the wave mode is its accessibility to the plasma core from the low density region. Stix[11] first derived a sufficient condition so that the wave index of refraction perpendicular to the magnetic field, $n_{\perp} = k_{\perp} c/\omega$, is real at all points between the antenna and the hybrid resonant layer. He concluded that this is the case if the index of refraction for the wave parallel to the magnetic field, $n_{//} = k_{//} c/\omega$, satisfies the condition

$$n_{//}^2 > 2 \left(1 + \omega_{pe}^2 / \omega_{ce}^2 \right) \quad . \qquad (2)$$

Briggs and Parker[12] and Golant[13], respectively, have made algebraic improvements and arrived at the less stringent conditions,

$$n_{//}^2 > 1 + (\omega_{pe}/\omega_{ce})$$

and

$$n_{//}^2 > 1 + (\omega_{pe}/\omega_{ce})^2 \qquad (3)$$

Troyon and Perkins[14] and Bers[15] have shown that upper bounds on $n_{//}$ of about 2 also exist. This upper bound is due to electron Landau damping or to a region of evanescence near the plasma edge. Thus in order to heat the core of the plasma an appropriate antenna array is required.

Bers[15] and Brambilla[16] have independently shown that a grilled launching structure providing wavelengths parallel to the magnetic field shorter than the free-space wavelength satisfies the necessary accessibility conditions. Bernabi, et al.[17] have provided the experimental verification of wave penetration with the launching guide array with the electric field in the split guide oriented parallel to the confining magnetic field. Recent experiments[18,19] on the Alcator and ATC plasmas have shown both effective launching of the waves and ion heating. The details of the heating mechanism appear to depend on nonlinear heating effects and are the subject of current research. It is thought that the ion heating is due to a nonlinear parametric decay of the pump wave into lower frequency hybrid waves and ion quasi-modes. This lower hybrid heating is of great current interest for present day machines due to its small waveguide array structure. Its applicability for penetration and heating of reactor size plasmas is less clear but certainly warrants further investigation.

The low frequency Alfvén waves ($\omega_{ci} >> \omega \sim k_{//}v_e$) have not been tested in a high power tokamak experiment since the electron Landau and transit-time damping are only appreciable at higher electron temperatures. Further, the launching efficiency is good only for large size devices such that the wave fields are not evanescent. Hasegawa and Chen[20] have considered resonant mode conversion

of the shear Alfvén wave $\omega = k_{\parallel} v_A(r)$ in a non-uniform plasma. In the collisionless hot electron limit ($T_e > 1$ keV), electron Laudau damping of the wave dominates the absorption process. Further, a strong enhancement of the wave magnetic field in the plasma compared to that applied in the vacuum region is predicted.

Messiaen and Vandenplas[21] have considered heating due to low frequency compressional magnetosonic wave bounded plasma resonances. They find that the plasma absorption by electron Landau damping greatly exceeds wall losses due to skin effect of the torus. In any wave heating scheme which heats electrons, one would have to rely on the energy equipartition time between electrons and ions being much shorter than energy confinement times. This is the case if current theories for energy confinement times are scaled up to larger machines of the reactor type.

Finally, considerable ECRH (Electron Cyclotron Resonance Heating) experience exists from the mirror program. However, the need for high power-high frequency sources (f ~ 100 GHz) has hampered heating studies for tokamak plasmas ($n \sim 5 \times 10^{13}/cm^3$) since for good penetration under ordinary ECRH circumstances the wave frequency must be larger than the electron plasma frequency. The modification of radial electron temperature profiles for tokamak discharges by means of this mode might be a means for reducing trapped particle diffusion losses. The gyrotron offers the possibility for utilization of this mode for tokamak plasmas.

3. Reactor Startup Utilizing Supplementary Fast Magnetosonic Wave Heating

In this section we consider a particular wave which may be used to ignite a tokamak reactor. Because of the potential for generation of large amounts of RF power, accessibility of the wave and energy deposition in the plasma core, and direct heating of the ions, we have decided to concentrate on the fast magnetosonic wave. Earlier theoretical works by Adam and Samain,[7] Perkins,[9] and Weynants[22] have presented the basic wave propagation properties and absorption mechanisms. The operative absorption mechanisms are cyclotron harmonic damping of the wave by the ions and Landau and transit-time damping of the wave by the electrons. Stix[23] has shown that when cross terms in the dielectric tensor are included in the electron damping calculation that for TFTR parameters the net electron damping is Landau damping and has a value which is half that for the transit time considered separately. We have found from computational studies that this is generally the case for reactor oriented machines.

We now present a brief derivation of the fast magnetosonic wave hot plasma dispersion relation. Assuming an $e^{-i\omega t + i\bar{k}\cdot\bar{r}}$ Fourier component of wave quantities, the wave equation is obtained as $\bar{k} \times (\bar{k} \times \bar{E}) + (\omega/c)^2 \bar{\bar{K}} \cdot E = 0$ where $\bar{\bar{K}}$ is the dielectric tensor as defined in Stix.[24] By noting that in the magnetosonic regime that the Bessel function argument $\lambda_j = k_\perp^2 \rho_j^2/2$ is small for both ion and electron terms, one can obtain a tractable dispersion relation in which first-order finite gyroradius effects are included by expanding to first order in λ_j. Further, the K_{zz} component of the dielectric tensor is so large compared to other elements involving the z component that the dispersion relation can be obtained to a very good approximation by expanding the 2 x 2 minor of the K_{zz} component. The dispersion relation then becomes ($k_\perp = k_x$, $k_{//} = k_z$) to the fourth order in $k_\perp$

$$\begin{vmatrix} (\omega/c)^2 K_{xx} - k_{\parallel}^2 & (\omega/c)^2 K_{xy} \\ (\omega/c)^2 K_{yx} & (\omega/c)^2 K_{yy} - k_{\parallel}^2 - k_{\perp}^2 \end{vmatrix} = 0 \qquad (4)$$

where

$$K_{xx} = 1 + \sum_{\alpha=i,e} (\omega_{p\alpha}^2/2\omega k_{\parallel} v_{\alpha})(Z_1^{\alpha} + Z_{-1}^{\alpha}) - k_{\perp}^2 \sum_{\alpha=i,e} (\omega_{p\alpha}^2 v_{\alpha}/4\omega k_{\parallel} \Omega_{\alpha}^2)(Z_1^{\alpha} + Z_{-1}^{\alpha} - Z_2^{\alpha} - Z_{-2}^{\alpha}),$$

$$K_{yy} = K_{xx} + k_{\perp}^2 \sum_{\alpha=i,e} (\omega_{p\alpha}^2 v_{\alpha}/\omega k_{\parallel} \Omega_{\alpha}^2)\,[Z_0^{\alpha} - 1/2(Z_1^{\alpha} + Z_{-1}^{\alpha})],$$

$$K_{xy} = -K_{yx} = -i \sum_{\alpha=i,e} (\omega_{p\alpha}^2/2\omega k_{\parallel} v_{\alpha})(Z_1^{\alpha} - Z_{-1}^{\alpha}) + ik_{\perp}^2 \sum_{\alpha=i,e} (\omega_{p\alpha}^2 v_{\alpha}/4\omega k_{\parallel} \Omega_{\alpha}^2)(2Z_1^{\alpha} - 2Z_{-1}^{\alpha} - Z_2^{\alpha} + Z_{-2}^{\alpha})$$

and Z_{ℓ}^{α} denotes the Fried and Conte Plasma dispersion function $Z((\omega + \ell\Omega_{\alpha})/k_{\parallel} v_{\alpha})$. The dispersion relation then includes wave absorption due to finite ion gyroradius effects, cyclotron damping, and electron transit-time damping (a factor of 2 greater than the resulting Landau damping obtained from the 3 x 3 dispersion relation).

The power absorbed by the ions and electrons per unit volume can be obtained in the weak damping limit in a manner following Stix[23] as $p = \omega \bar{E}^* \cdot (\bar{\bar{K}}^a \cdot \bar{E})/2 (\text{watt/cm}^3)$ where $\bar{\bar{K}}^a$ is the anti-Hermitian part of the dielectric tensor. The finite ion gyroradius damping terms becomes

$$P_i = \pi^{1/2} \varepsilon_0 \omega_{pi}^2 (Re\lambda_i)^{\ell-1} |E_+|^2 e^{-((\omega - \ell\omega_{ci})/k_{\parallel} v_i)^2} / 4k_{\parallel} v_i \qquad (5)$$

and the electron Landau damping term can be written

$$P_e = \pi^{1/2} \varepsilon_0 (\omega_{pe}/\omega_{ce})^2 k_{\perp}^2 |E_y|^2 v_e e^{-(\omega/k_{\parallel} v_e)^2} / 4k_{\parallel} \qquad (6)$$

In the above equations, ℓ is the harmonic number $\omega = \ell\omega_{ci}$, E_+ is the left-hand circularly polarized electric field component rotating in the sense of the ions,

and E_y is the rectangular component of the electric field. $|E_+| = |1-\chi||E_y|$, where $\chi = iE_x/E_y$ is the polarization factor.

The ion cyclotron harmonic absorption term occurs in a region of finite width in the tokamak minor cross section due to the thermal effects and the 1/R variation of the toroidal magnetic field. For the second harmonic, this width is $\Delta = k_{||} v_i R/\omega_{ci}$. It is further assumed that the energy deposited in the slab is uniformly distributed over the circular flux surface intersecting the radial element on the slab due to the rotational transform. After making this calculation, one can obtain the variation of the ion heating profile with plasma radius as

$$\langle p_i \rangle = \varepsilon_o(\omega_{pi}^2/\omega_{ci})(R/r)\ \mathrm{Re}(\lambda_i)^{\ell-1}|E_+|^2/4\ell \qquad (7)$$

where the brackets indicate that it has been averaged over the flux surface. Note that this provides a strong peaking of the energy deposition to the ions at the plasma core. By integration over the tokamak cross section these equations are adapted to a time-dependent model for the startup calculation in UWMAK-III.

The last point is the existence of toroidal eigenmodes for the tokamak as predicted by Adam and observed experimentally on ST.[3] These modes are beneficial in that they enhance the plasma loading of the wave launching structure and allow efficient heating of the plasma. Indeed, in smaller devices such as ST, the eigenmodes are well separated but for large reactor machines such as UWMAK-III the density of toroidal eignemodes in the frequency domain becomes a near continuum. Stix,[23] Swanson and Ngan,[25] Scharer et al,[26] and Mau et al.[27] have indicated that when toroidal, poloidal, and radial eigenvalues are varied, the spacing between modes may be as small as one part in 60,000 of the magnetosonic wave frequency. This means that eigenmodes will always be available to

heat the plasma but the cumulative effect of all excited modes on the loading of the launching structure and heating efficiency is a subject which will require much further study before a conclusion can be reached. Swanson and Ngan[25] have indicated that the overlapping density of eigenmodes enhance the mode conversion to ion Bernstein modes but Scharer et al.[26] and Mau et al.[27] have shown that the introduction of large $k_{//}$ in the wave can minimize this effect. Figure 3-1 shows a plot of the dispersion relation for the fast magnetosonic (F) and ion Bernstein (B) wave modes in the neighborhood of resonance ($f = 2f_{CD} = 60$ MHz @ 40 kG) for a plasma with $n_e = 2n_D = 2n_T = 1.2 \times 10^{14}/cm^3$ and $T_D = T_T = T_e = 6$ keV. This corresponds to conditions just before the RF is turned off and α-particle heating drives the plasma to the reactor operating conditions. For $k_{||} = 0$ the roots for $\lambda_i = k_\perp^2 \rho_i^2/2$ coalesce in the region between $1.95 < \omega/\omega_{CD} < 2.00$ where mode conversion can occur. This means that some of the wave power incident on the fast wave branch is mode converted to ion Bernstein wave energy. The wave energy can be kept predominantly in the fast wave mode by increasing the $k_{//}$ of the wave so that the region of conversion is minimized and the fast wave tunnels through. Figure 3-2 shows the effect of increasing $k_{||}$ to $5m^{-1}$ for the same plasma parameters. It is seen that the roots are much more separated so that tunneling by the fast wave occurs. An increase in $k_{//}$ separates the modes still further.

Thus, the heating rates used in this startup calculation might be considered as a simplistic model with the details of wave penetration due to plasma profile effects at the edge, the influence of the dense eigenmode structure, and the resultant velocity distributions of heated particles on the net heating rates subjects of further investigation.

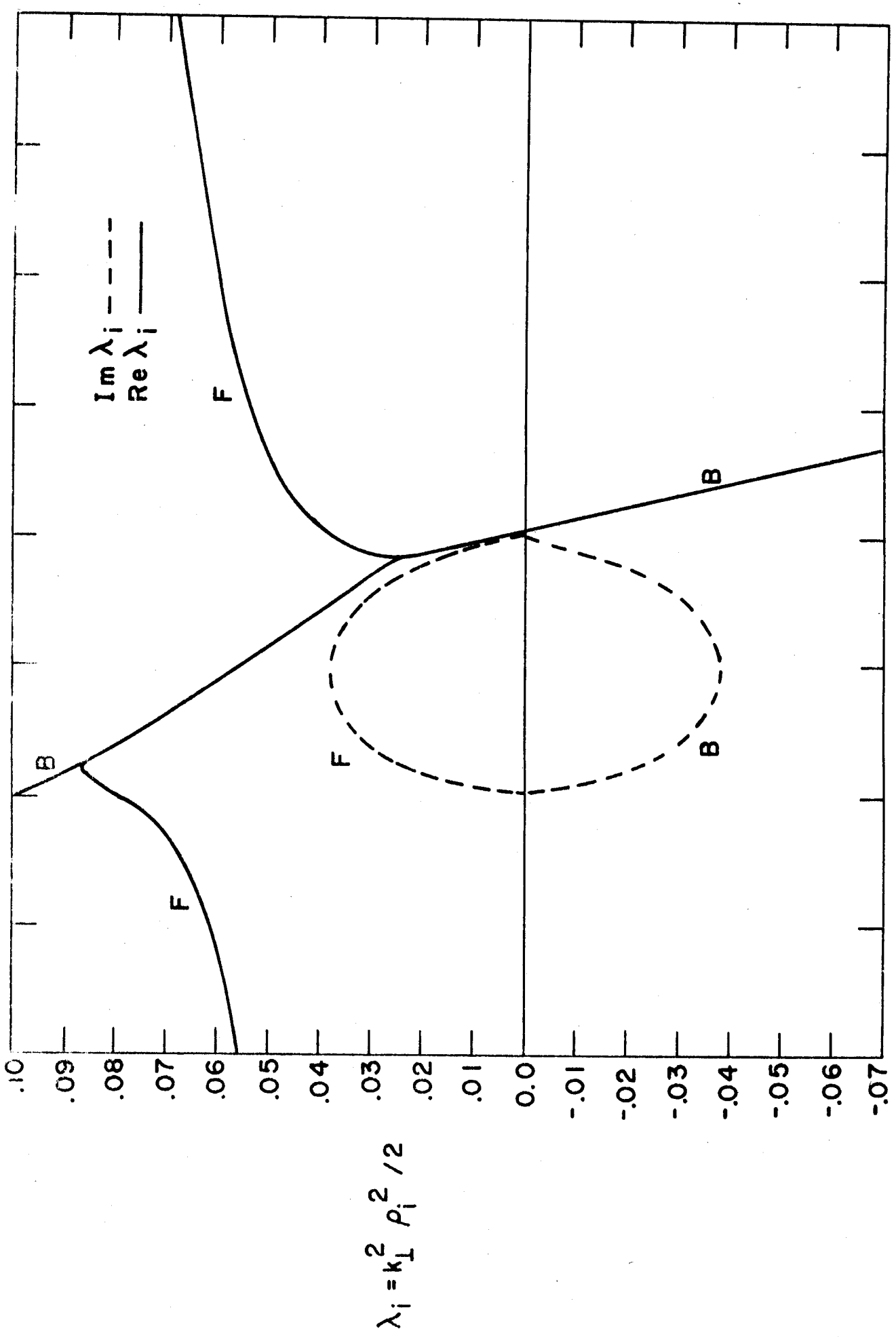

Fig. 3-1 Dispersion relation for $k_{//} = 0$

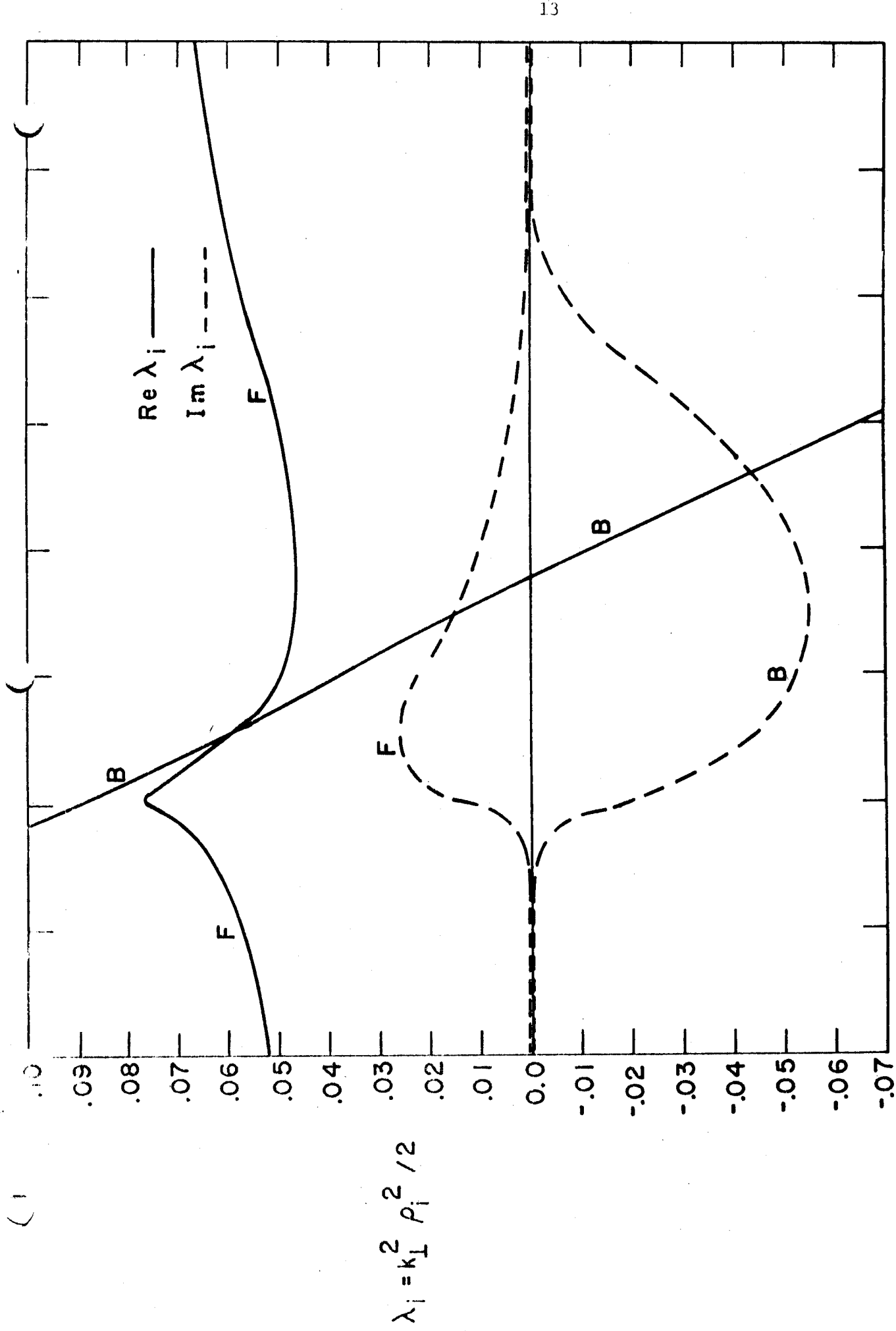

Fig. 3-2 Dispersion relation for $k_{\parallel} = 5\ m^{-1}$

To calculate the heating rates, we simultaneously solve both electron and ion energy balance equations. A global balance model similar to the one used for UWMAK-II calculations[28] was modified to account for the noncircular plasma in UWMAK-III.[29] In addition the plasma was assumed to be impurity free and microinstability theory was used to calculate the transport coefficients.

The basic energy conservation equation for the ions is

$$\frac{d}{dt}\left(\frac{3}{2} n_i \kappa T_i\right) = W^i_{RF} + W^i_{PF} + W_{ei} - W^i_E \qquad (8)$$

where

W^i_{RF} is the fraction of injected power deposited in the ions

W^i_{PF} is the fraction of alpha energy from thermal plasma fusions deposited in the ions

W^i_{ei} is the energy loss rate due to electron-ion rethermalization

W^i_E is the energy loss rate due to transport processes.

For the electrons we have

$$\frac{d}{dt}\left(\frac{3}{2} n_e \kappa T_e\right) = W^e_{RF} + W^e_{PF} + W_{ohmic} - W^e_E - W_{RAD} \qquad (9)$$

where the various terms now refer to the electrons and where W_{RAD} are the radiative losses. Equations (8) and (9) written in cylindrical coordinates become

$$\frac{\partial n_e T_e}{\partial t} = 4.28 \times 10^{-11} n_e n_i \frac{(T_i - T_e)}{T_e^{3/2}} + \frac{1}{1.5r}\frac{\partial}{\partial r}\left(r n_e \chi_e \frac{\partial T_e}{\partial r}\right) - \frac{1}{r}\frac{\partial}{\partial r}\left(r n_e v_e T_e\right)$$

$$+ 4.17 \times 10^{15} \left\{n_D n_T \langle \sigma v \rangle_{DT} U_{\alpha e} + \underline{E} \cdot \underline{J} + P_{Te} - P_I - P_B - P_S - P_L - P_R\right\} \qquad (10)$$

and

$$\frac{\partial n_i T_i}{\partial t} = -4.28 \times 10^{-11} n_i n_e \frac{(T_i - T_e)}{T_e^{3/2}} + \frac{1}{1.5r}\frac{\partial}{\partial r}\left(r n_i \chi_i \frac{\partial T_i}{\partial r}\right) - \frac{1}{r}\frac{\partial}{\partial r}\left(r n_i v_i T_i\right)$$

$$+ 4.17 \times 10^{15} \{n_D n_T \langle\sigma v\rangle_{DT} U_{\alpha i} + P_{ti}\} \qquad (11)$$

$T_{e,(i)}$ is the electron (ion) temperature (eV), B_θ is the poloidal magnetic field (gauss), $n_{e,(i)}$ is the electron (ion) density (cm^{-3}), $v_{e,(i)}$ is the electron (ion) velocity (cm/ms), J is the toroidal current density (amp/cm^2), E is the toroidal electric field (volt/cm), r is the radius (cm), t is time (ms), $\chi_{e,(i)}$ is the electron (ion) thermal diffusivity (cm^2/ms), and $U_{\alpha i,(e)}$ is the fraction of alpha energy going to ions (electrons). P_B, P_S, P_L and P_R represent bremsstrahlung, synchrotron, line and recombination radiation, respectively (watts). $P_{te(i)}$ is the total amount of rf power going to the electrons (ions) in watts. Expressions for P_S, P_L, P_R and for the conduction and convection terms may be found in Ref. (29).

The other terms are evaluated by assuming a parabolic profile for both the temperature and the density. The average density is calculated from

$$\bar{n} = \frac{2\int_o^a n(r)\, r\, dr}{a^2} \qquad (12)$$

while the average temperature is calculated from

$$\bar{T} = \frac{\int_o^a n(r)\, T(r) r dr}{\int_o^a n(r)\, r\, dr} \quad . \qquad (13)$$

What remains to be done is to calculate the RF heating terms P_{te} and P_{ti}.

We now adapt the heating equations from the previous section to a time dependent model of heating at the second harmonic of the deuteron ion cyclotron frequency. For the ions we assume a parabolic density and temperature profile given by

$$n_i = 2n_o(1-(r/a)^2) \text{ and } T_i = 2T_o(1-(r/a)^2)$$

where a is the plasma radius. By integrating eq. (7) over the plasma volume we can determine the power delivered to the ions as

$$P_{ti} = \int \langle p_i \rangle r \, dr \, d\theta \, dz$$

$$P_{ti} = \frac{((4.84\times10^{-11})n_o R)T_o^2 a|E_+|^2}{B_o^3} \text{ watts} \qquad (14)$$

where B_o is in Gauss, T_o in keV, n_o in cm^{-3} and $|E_+|$ in V/m which is assumed uniform over the cross section.

For the electron heating we assume a density and temperature profile for the ions as given above and for the electrons given by

$$n_e = 2n_1(1 - (r/a)^2) \text{ and } T_e = 2T_1 (1 - (r/a)^2).$$

The electric field polarization is related by

$$E_y = E_+(1 + 6.94 \times 10^{-23} n_i^2 T_e B_o^{-2}) \qquad (15)$$

where T_e is measured in keV, n_i in cm^{-3} and B_o in Gauss.

The electron power absorption per unit volume becomes

$$p_e = (8 n_o n_i e^2 |E_+|^2/\epsilon_o B_o^2 Mc^2 k_{//})(\pi m \kappa T_1)^{1/2} \exp\left[\frac{-2 e^2 B_o^2 m}{k_{//}^2 \kappa T_e M^2}\right] \times$$

$$\left[(1-r^2/a^2)^{5/2} + \frac{5.53\times10^{-19}(1-(r/a)^2) n_o T_o}{B_o^2}\right] \text{ (watts/cm}^3\text{)}. \qquad (16)$$

We then integrate this over the plasma volume, inserting the average electron temperature over the cross section in the exponential Landau term and obtain

$$P_{te} = 3.28\times10^{-26} n_o n_1 |E_+|^2 T_1^{1/2} \exp[-6.64\times10^{-9} B_o^2 T_1^{-1}] Ra^2 B_o^{-2} \quad \times$$

$$\left[\frac{1}{7} + \frac{5.53\times10^{-19} n_o^2 T_o}{13\ B_o^2} \right] \text{ watts} \qquad (17)$$

where T and a are measured in cm.

Figure 3-3 shows a cross sectional view of the UWMAK-III reactor.[29] The average density is 6 x $10^{13}/cm^3$ with a magnetic field of 40 kG and a major radius of 8.1 m. At the end of the 15 sec ohmic heating phase, the electrons and ions reach a temperature of 1.8 keV. At the end of the ohmic heating cycle, the magnetosonic wave heating is turned on. Although dominant heating of the perpendicular ion velocity is expected, a Maxwellian heating is assumed consistent with the global model. We first consider a constant injected power of 40 MW, most of which is deposited with the ions. Fig. 3-4 illustrates the ion and electron temperatures during the startup cycle. After 8 seconds the plasma reaches ignition where the α-particle heating exceeds the energy losses. If the injected wave power is left on for 12 secs, the plasma reaches the equilibrium temperature of T_i = 19 keV and T_e = 23 keV in 15 secs.

CROSS SECTION VIEW OF UWMAK III

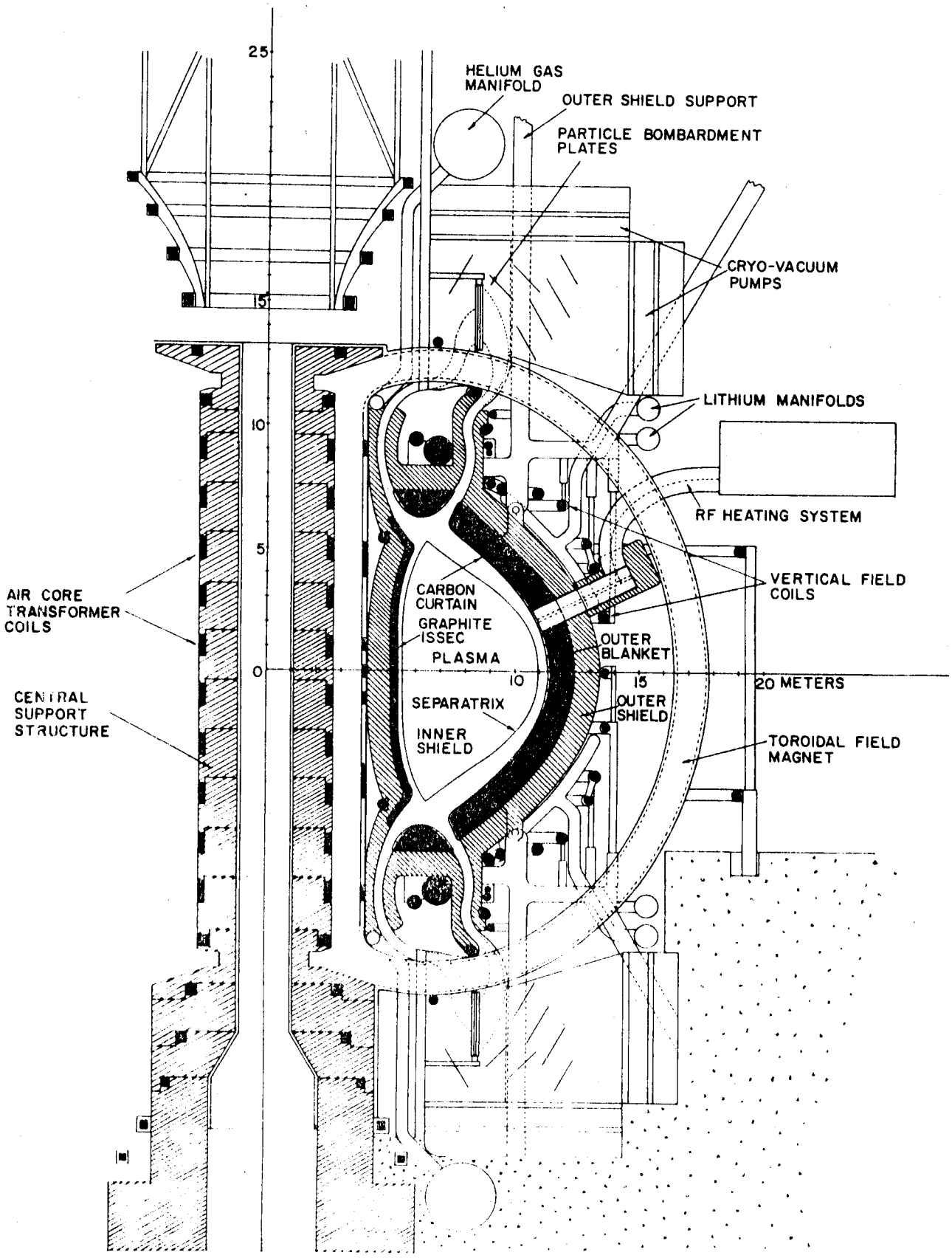

Fig. 3-3

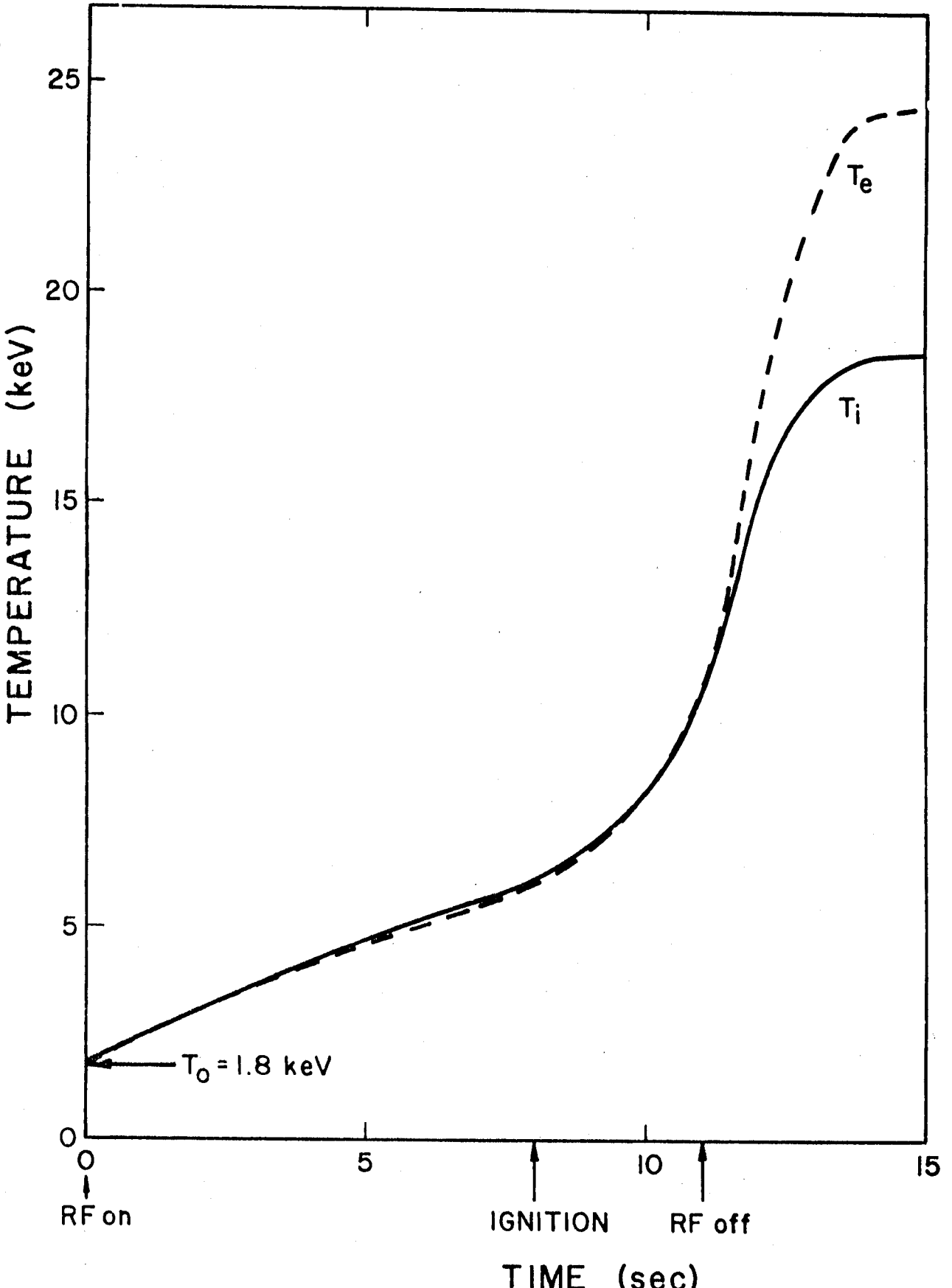

Figure 3-4 - Magnetosonic Wave Heating to Reactor Operating Conditions
P_{RF} = 40 MW

As an alternative case, we consider a constant heating power of 200 MW. Fig. 3-5 shows that ignition is reached after 1.32 secs and the magnetosonic wave heating is turned off after 1.36 sec. In this case, the ions are driven to a temperature 450 eV greater than that of the electrons during the magnetosonic wave heating phase. It can be seen that the ions begin to cool after extinguishing the supplementary heating but the alpha heating contribution is larger than the loss terms so that the plasma continues to heat and reaches equilibrium in 15 secs. In this case, it is important that the ions are heated sufficiently greater than the electrons so that during the drop in ion temperature, the plasma continues to heat and reach reactor equilibrium.

In both cases, the net energy given to the plasma by the magnetosonic wave heating system is within a factor of 2. Even though the ions absorb most of the heating power, the ion-electron equilibration time is sufficiently short so that the electron temperature follows the ion temperature to ignition. Only if there is a mechanism which destroys the ion heating by the electrons would it be necessary to consider plasma heating which deposits its energy within the ions with the present trapped particle scaling laws.

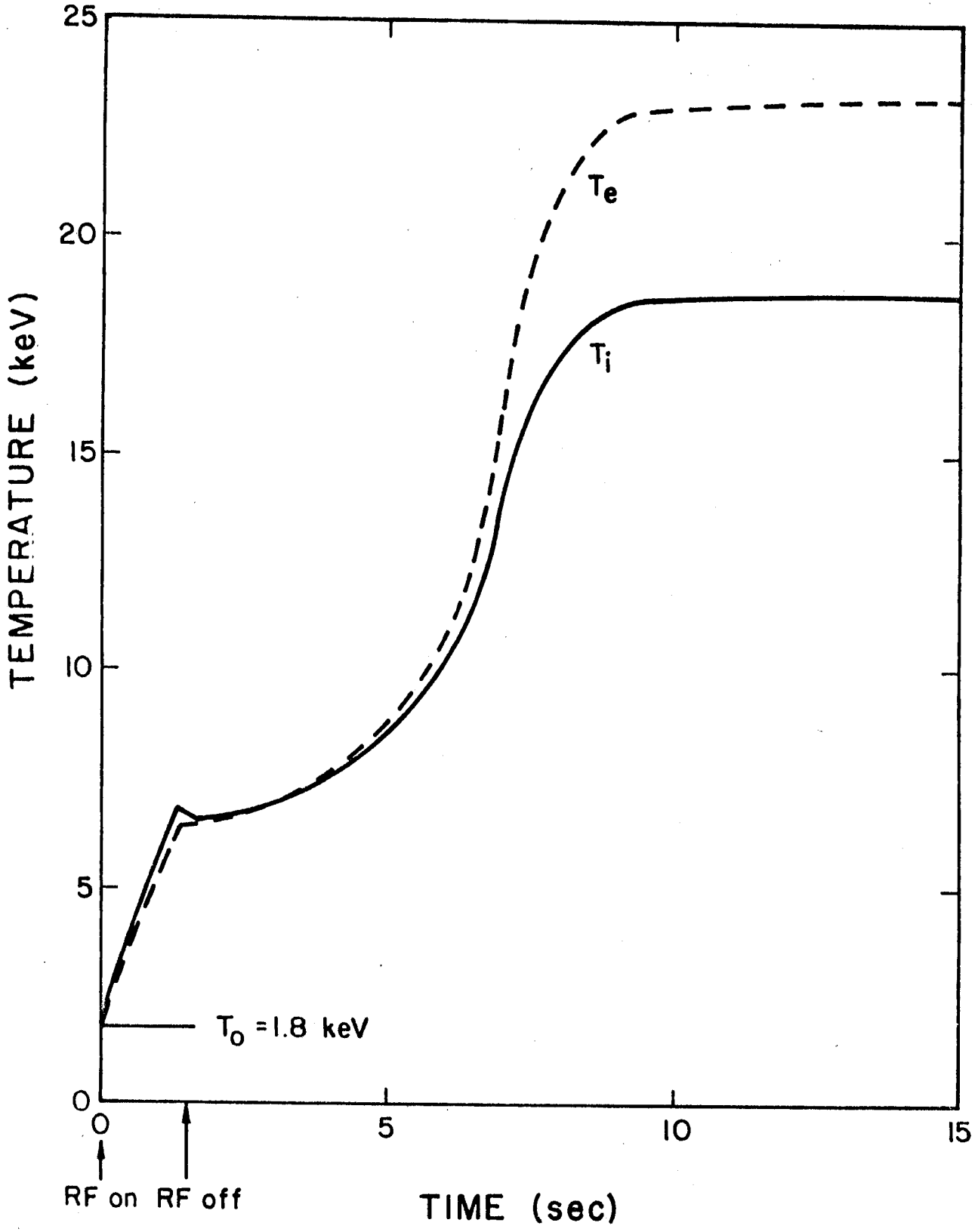

Figure 3-5 - Magnetosonic Wave Heating to Reactor Operating Conditions P_{RF} = 200 MW

4. Conceptual Magnetosonic Wave Launching System

In order to heat the plasma by fast magnetosonic wave eigenmodes, a suitable launching structure located in the torus wall must be devised. It must be capable of handling 200 MW of power at 60 MHz for a startup period of 15 seconds. It must have the property that the RF fields excited have a toroidal magnetic field with an orthogonal electric field as shown in Fig. 4-1a. It must also excite desirable modes which lead to energy deposition near the plasma core. An ideal system would have a spectrum which excites lower order poloidal m values since higher order m values cause the finite ion gyroradius heating to peak further towards the plasma edge, leading to edge heating rather than core heating. In order to excite only low m numbers, the source distribution would have to cover most of the poloidal circumference. A further problem is caused by the fact that for large tokamaks such as UWMAK-III, the minor circumference is large compared to a free space wave length $2\pi a > \lambda_o$. This introduces phase shifts of a wave traveling in the poloidal direction which contribute to a higher order poloidal spectrum and reduced efficiency. A possibility for overcoming this is to introduce external circuit phase shifts which correct for the natural phase shift of the wave as it travels in the poloidal sense.

A further possible plasma consideration in the design of the launching system is the fact that many eigenmodes can be excited at a given frequency. Weynants[30] and Swanson and Ngan[25] have indicated that magnetosonic wave modes propagating towards the core from the high field region can undergo mode conversion reflected power from the plasma back towards the source. Scharer et al.[26] and Mau et al.[27] have shown that the region of confluence between the fast magnetosonic mode and the ion Bernstein mode can be made very small by the excitation of modes with $k_{\parallel}$ sufficiently large compared to the free space wave number k_o. This can minimize the mode conversion from the magnetosonic wave. Further, as shown in

eqn. (6), the relative amount of electron Landau damping obtained by the magnetosonic mode can be increased by making $\omega/k_{//} v_e \sim 1$. Thus, if startup requires a more detailed consideration of the wave modes' initial deposition of energy to the ions and electrons, the potential of varying the wavenumber parallel to the magnetic field provides a possibility for tuning the relative energy deposition to ions and electrons. A drawback of the higher $k_{//}$ excitation spectrum is that the field intensity between the torus wall and plasma edge will be evanescent causing a reduction in heating efficiency. Cato et al.[31] have considered a poloidal hoop to excite RF fields in a tokamak reactor. The hoop would have to be made from a series of short sections driven to provide uniform phase excitation in the poloidal sense as shown in Fig. 4-1c. The main problems that have to be worked out are the impurity contribution caused by its proximity to the discharge and the required coaxial insulators.

A standard rectangular waveguide launcher flush mounted in the wall as shown in Fig. 4-1b introduces new spectral excitation problems since its toroidal dimension must be larger than half a free space wavelength for propagation of the dominant TE_{10} mode. As noted in the later sections, this can be overcome by using an array of smaller waveguides, possibly filled with high dielectric ceramic which reduces the dimension of the guide and excites larger $k_{//}$ values. If a small excursion of conducting material into the torus can be tolerated, a strip line located over ceramic dielectric inside a rectangular guide could be envisioned which does not have a cut-off limitation due to small aperture size. The conducting strip would have to be coupled to the torus by making a small loop which is electrically connected to the bottom of the guide.

The constraints on the design of the RF power system are as follows: It is assumed that up to 200 MW are provided by as many as sixteen separate feed

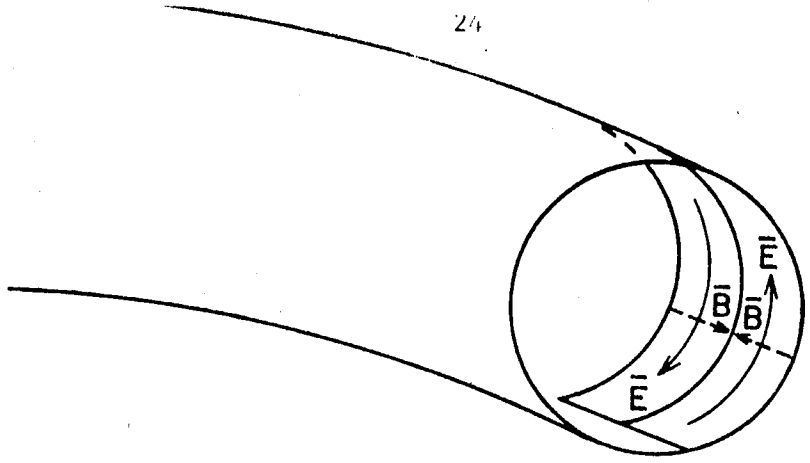

a) IDEALIZED MAGNETOSONIC WAVE FIELD SOURCE DISTRIBUTION:
$k_{||}$ = 6-10 m^{-1} AND DOMINANT $m = 0, \pm 1, \pm 2$ EXCITATION

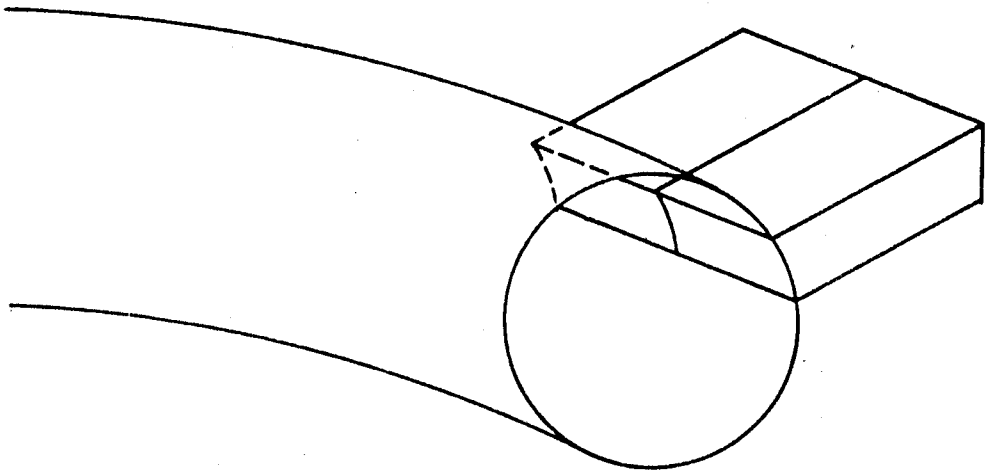

b) EXCITATION BY MEANS OF STANDARD WAVEGUIDES

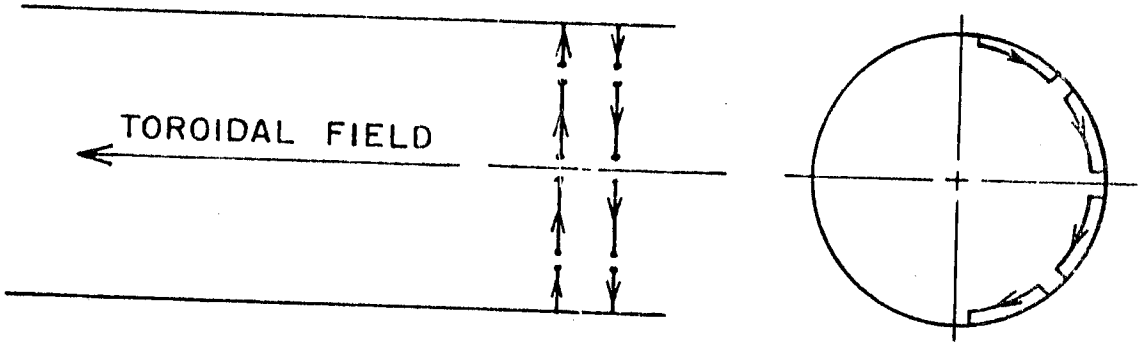

c) HOOP EXCITATION

Figure 4-1 - Considerations for Magnetosonic Wave Heating Launching Structure

systems with a minimum capability of 13 MW/feed. These feeds are placed in pairs located poloidally around the device. A single unit is shown in Fig. 3-3 This puts a constraint on the minimum cross-sectional area of the feed so that the field strengths remain below the breakdown level. While the magnitude of electric field strengths for 60 MHz breakdown in a tokamak environment is not precisely known, several estimates are indicated in the literature. Hooke et al. have indicated privately that a 25 MHz, 10 kV/cm RF field on ST did not give rise to breakdown while Weynants [30] assumes a maximum field strength of 30 V/cm in the plasma in his magnetosonic wave heating calculations. In UWMAK-III, we adopt the criteria that the RF field be held to a maximum of 3 kV/cm in the RF feeds during startup. It would be preferable if the startup neutral pressure outside the plasma confinement region was below 10^{-5} Torr, but 10^{-4} Torr is all that can be accomodated given the large device size, pumping capacity and limited pumping area.

A further condition that will require considerable theoretical and experimental effort is the plasma loading impedance on the launching structure. Of particular interest is the effect of a near continuum of eigenmodes excited at different levels on the input impedance. A simplified model indicates that the input resistance related to absorption mechanisms for the modes will effectively be in parallel, indicating a low value for the resistive part of the input impedance. If the wave impedance of the RF feeds is low, this will allow a more easily obtained match for the supplementary heating system to the plasma. Both ridged waveguide and dielectric filling contribute to a reduction in the wave impedance in the RF feed system.

Another aspect of the generation of 60 MHz RF power at 10 MW levels is the necessary development. A small to moderate development would be required

to advance the state of RF generation from current 1 MW CW levels/tube to 10 MW levels. Other problems would involve details of the matching and feed design that could be incorporated in the UWMAK-III configuration.

The design of the waveguide feed is obtained subject to the following conditions: (1) each element of the launching structure must be capable of supplying 13 MW of power with a maximum electric field strength of 3 kV/cm. (2) The ratio of wave frequency to cutoff frequency of the feed must be greater than 1.2 in order that the attenuation in the guide due to skin effect is not too large. If we require that the feed be a vacuum region then one can consider two types. In all cases due to a lower cost of fabrication, it is advisable to consider a copper coaxial line running most of the distance from the RF source to the torus with a 1 m diameter. A coaxial to waveguide transition could be made near the torus wall.

If the neutron and plasma flux to the launching aperture during startup dictate a vacuum filled waveguide, the following designs can be considered. A rectangular guide with a ratio of wave frequency to cutoff frequency of $f/f_c = 1.2$ for the TE_{10} mode. This would require a toroidal inner dimension of 3 m and a poloidal dimension of 1.5 m as shown in Fig. 4-2a. A waveguide of this size with the imposed maximum field intensity of 3 kV/cm would have a theoretical power injection energy capability of 500 MW and a wave impedance of 190 ohms. In order to reduce the toroidal extent of the guide for improved wave penetration and heating, a ridged waveguide[32] can be considered. This reduces the mode conversion potential and provides a means of determining the fraction of wave power initially deposited in the ions vs the electrons. The H-shaped guide would have the inner dimensions of 1 m high by 1 m wide with a

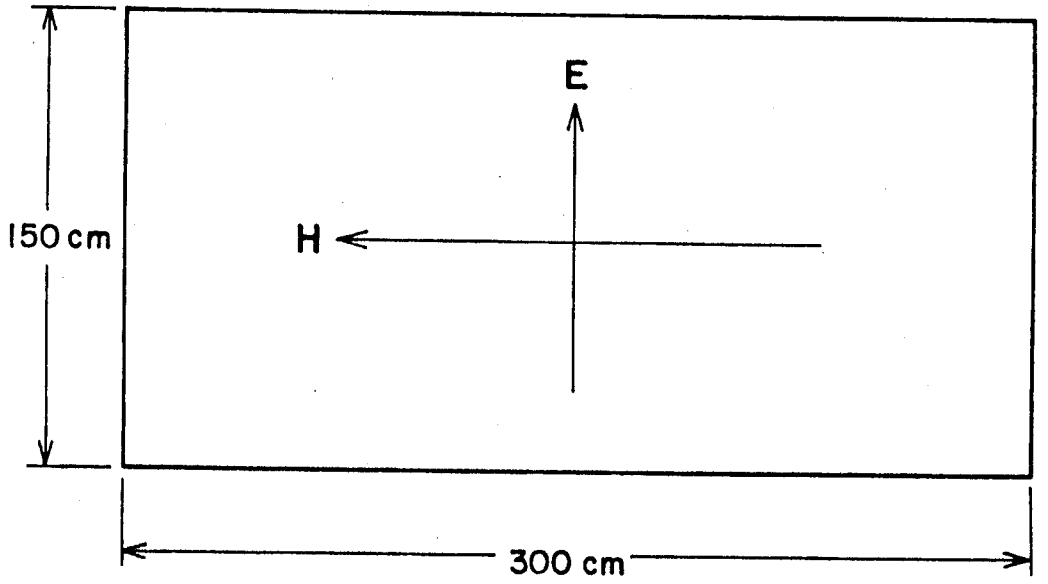

a) STANDARD RECTANGULAR WAVEGUIDE

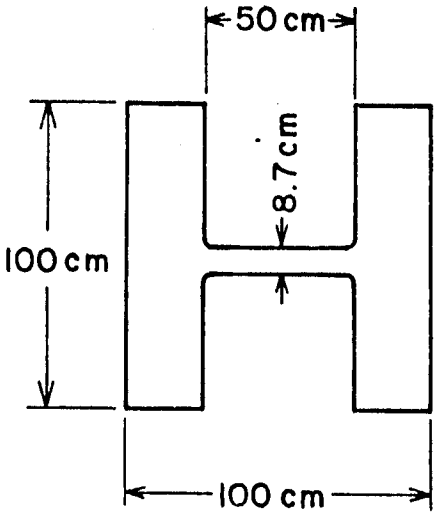

b) RIDGED WAVEGUIDE

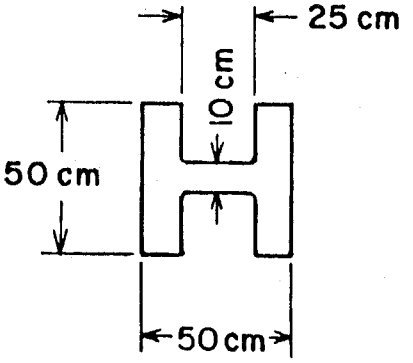

c) RIDGED WAVEGUIDE WITH CERAMIC ($\epsilon_r = 8$) FILLED DIELECTRIC

Figure 4-2 - Size Comparisonof TE_{10} Waveguide Feeds For 60 MHz RF

gap width of 8.7 cm which is 50 cm in extent as shown in Fig. 4-2b. The wave impedance of the dominant TE_{10} mode is 70 ohms and the theoretical power carrying capability is 30 MW.

If neutron and plasma heating of the guide aperture during startup are not too severe, a guide which is partially or fully filled with a dielectric medium can be considered. Alumina ceramic (Al_2O_3) has a relative dielectric constant of $\varepsilon_r = 8$, a loss tangent of 10^{-4}, and a maximum temperature of operation of 1500-1900°C. A ridged waveguide which is filled as shown on Fig. 4-2c. The wave impedance is 40 ohms and a theoretical power transfer of 60 MW can be obtained.

Under UWMAK-III reactor operating conditions the neutral and charged particle flux to the wall is about 10^{14} particles/cm^2-sec and corresponds to a wall loading of 2 MW/m^2. One might envision a 1m thick movable shield that is placed in front of the waveguide ports after the supplementary heating to ignition. If a shield cannot be considered and the feed is exposed to neutron bombardment, a ridged guide fabricated of molybdenum and lithium cooled operating at ~800°C can be envisioned. Molybdenum has a high conductivity (2×10^5 mhos/cm @ 20°C) comparable to copper and is capable of operating at high temperatures. Its conductivity is about six times lower at an operating temperature of 800°C and it is expected to have little change in conductivity due to neutron bombardment.

It is evident from previous considerations that several alternatives for the design of magnetosonic wave launching structures exist. Much further work in relating a given wave source on the torus wall to the heating deposition profiles in the plasma is required. From the plasma point of view, a wave source that goes half way around the minor cross-section on the outside edge is required. A second source located close to the first but shifted in phase by 180° is proposed in order to set up sufficiently short wavelengths ($\lambda \sim 1$ m) in the toroidal sense in order to minimize mode conversion of the fast wave.

5. Neutral Beam Injection Heating of Tokamaks

At the present time, the injection of high energy neutrals into plasmas is the primary auxiliary heating method in tokamaks and the primary fueling mechanism in mirror machines. Generally, the problem can be divided into three areas: source development; beam transport system to the plasma; and beam-plasma interactions. By analogy, the three comparable areas for RF heating are the RF generator, the access and launching structure, and wave-plasma interaction.

a. Overview of Status of Neutral Beam Development

High powered neutral beam sources for fusion reactor application remains an area where significant technological development remains. Present day sources are capable of delivering up to 250kW at up to 40 keV for roughly 200ms.[33,34] Near term sources planned for the future are to deliver between 1 and 3 MW of power at 120 to 150 keV for times on the order of 500 ms to 1 s.[35,36] An example of the design of the Oak Ridge type[35] is shown in Fig. 5-1. As we will show and as has been discussed elsewhere,[37] reactor systems will require at least 200 keV deuterium beams capable of delivering 10-20 MW per module for times of between 1 and 10 s. Beam driven reactors, such as the tokamak engineering test reactor[38] or tokamak hybrids,[39] will require similar beams capable of continuous operation and with efficiencies of 50% or higher.

The development of high power, high energy, and high efficiency neutral beam injectors requires that we learn to deal with the problems of thermal limitations on the accelerating grids, arcing, scattering of ions and electrons in the gap between electrodes, secondary electron emission, gas flow and vacuum pumping. For example, the electrodes will have to be cooled to prevent thermal distortion. In addition, the spacing between electrodes is limited by space charge blowup of the beam and by arcing. The space charge limit is given by Child's law,[40]

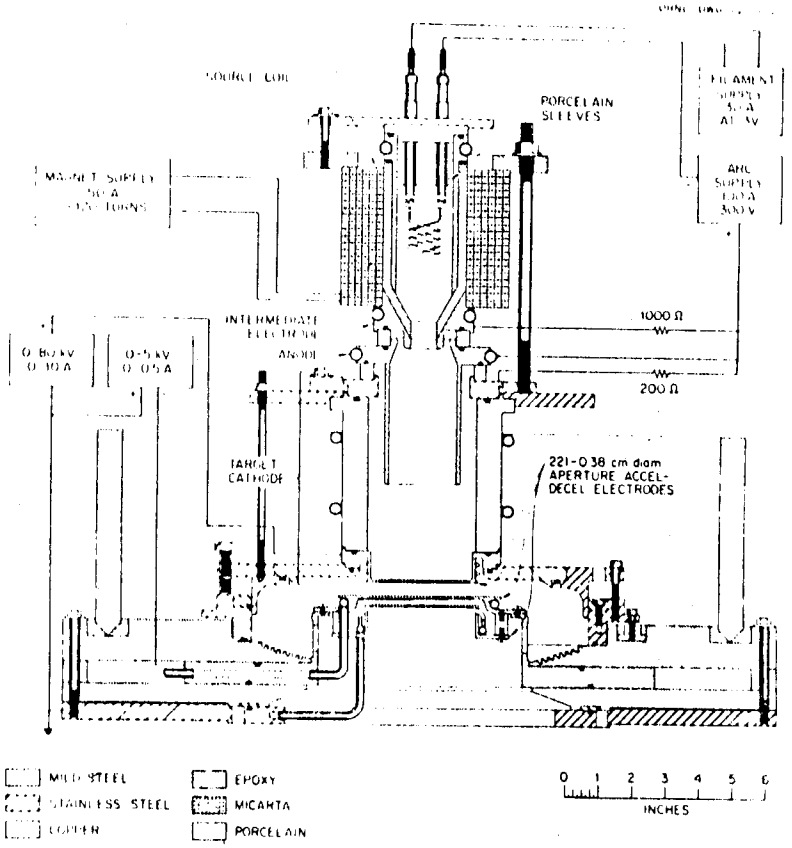

Fig. 5-1 - DuoPIGatron Ion Source and Accel-Decel Extraction System of Oak Ridge Design. From ref. 35

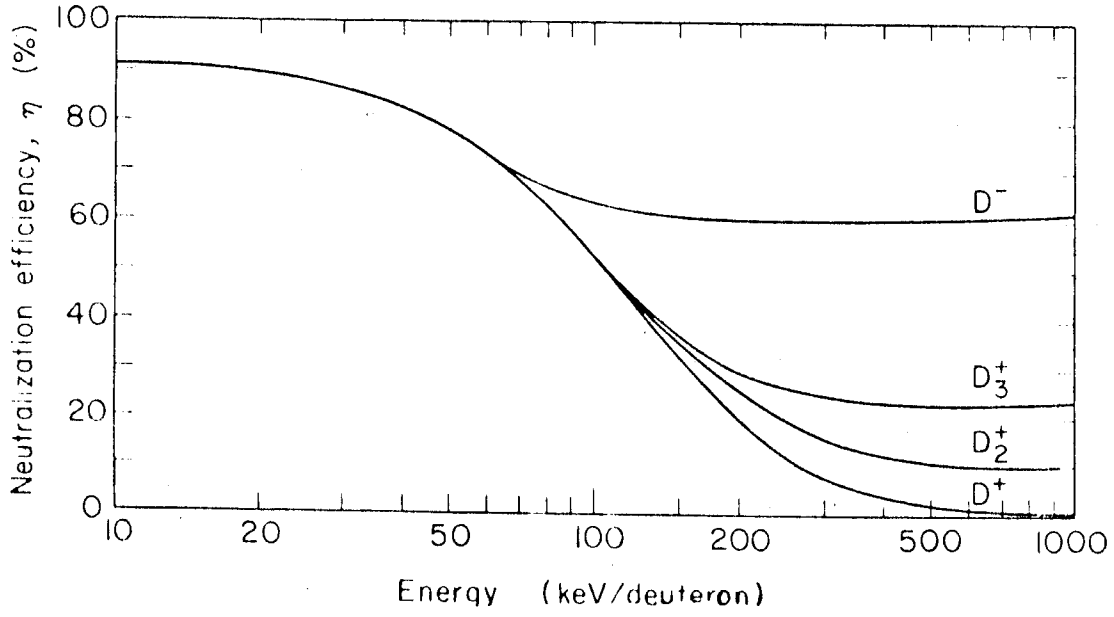

Fig. 5-2 - Maximum neutralization efficiencies calculated by Beckner, Pyle, and Stearns[11] in D_2 versus beam energy, for D^+, D_2^+, D_3^+, and D^- beams.

$$j \leq \frac{C_1 V^{3/2}}{\sqrt{A}\, \chi^2} \tag{18}$$

where V is the voltage, A is the atomic mass of the beam atoms, χ is the spacing between electrodes and C_1 is a constant. This is for a single stage system. Also, the critical voltage to prevent arcing has been found to vary as the $\sqrt{x}$.[41] As such, the limitation on current density follows the formula

$$j \leq \frac{C_2}{\sqrt{A}}\, V^{-5/2} \tag{19}$$

i.e. as the accelerating voltage increases, the extracted current density decreases. Thus, to achieve high powers will require large aperture beam systems.

It is possible to relieve this problem somewhat by going to multistaged acceleration.[42] All plans for high power, high energy sources do indeed plan for multistage acceleration. However, the technology here is far from being fully demonstrated. An example of the problem was pointed out by Hamilton et al.[36] At present, available source current densities are about 300 mA/cm^2 for D^+ and 100 mA/cm^2 for D_2^+ and D_3^+. For D^-, which is desirable for efficient high energy injection, the presently achieved current density is only about 12 mA/cm^2. For reactors we are going to require 1-3 A/cm^2 in order to keep the overall beam size small (so beam lines will fit onto the machines) and to reduce the gas load. 1 to 2 A/cm^2 represents an extrapolation of between 30 and 300.

The gas flow and pumping requirements relate to the source gas efficiency (the ratio of ions extracted from the source to the gas feed rate) and to the neutralizer cell. At the moment, typical[35,36] source gas efficiencies are

about 30% which means for 1 A of extracted ions, the gas feed rate is 3.3 A equivalent and the neutral gas not extracted as ions passes through the system into a neutralizer cell.

In addition, not all ions extracted from the source are monatomic.[43] For positive ion sources, which are the most highly developed today, the monatomic species ranges from 50%[35] to 75%[36] of the ion beam. For the LBL sources, the breakdown is; 75% D^+, 15% D_2^+, 10% D_3^+ in deuterium; 60% H^+, 20% H_2^+ and 20% H_3^+ in hydrogen. This is clearly very important because the half and third energy components, upon breakup, do not penetrate plasmas as well and will tend to be deposited near the edge. In addition, the lower energy fast ions are more susceptable to charge exchange which will in turn lead to fast neutrals that can escape the plasma and cause sputtering of the first wall. This problem has been extensively studied for two component tokamaks[45] and will be discussed further as we proceed.

After passing through the accelerating stages, the fast atomic and molecular positive ion beam is passed through a neutralization cell, typically H_2 or D_2 gas depending on the beam. Berkner, Pyle, and Stearns[43] have calculated the neutralization efficiency for D^+, D_2^+, D_3^+ and D^- beams as a function of energy per deuteron and their result is shown in Fig. 5-2. For the energy per deuteron less than 75 keV, positive ion sources can give neutralization efficiencies of up to 90% but more typically the value would be 60-70%. The unneutralized beam escaping the neutralizer cell is removed by magnetic deflection to a beam dump. The drift tube from the neutralizer to the plasma is differentially pumped to minimize the gas flow to the plasma and to prevent

collisions of the fast neutrals with background gas.

At higher energies, positive ion beams become less efficient and there is strong incentive to go over to negative ion sources and to use direct conversion on the unneutralized portion of the beam. Both these problems require substantial technological development. To date, no high power, high voltage negative-ion based neutral beam system has been produced. The incentive for negative ion sources is, as shown in Fig. 5-2, the fact that neutralization efficiencies can exceed 70% for beam energies of as much as 1 MeV. Two approaches still in the early stages of development are the direct extraction of D^- from the source and the use of an alkalai vapor cell,[45] such as cesium, to convert a low energy positive ion beam to a low energy negative ion beam which is then accelerated and neutralized. The conceptual design of a system based on cesium vapor cells was discussed by our group in Ref. 46. The design was for a 500 keV D° neutral beam system. It starts with a 1.5 keV D^+ beam produced by a scaled version of a duoPIGatron.[33] This beam is injected into 10 equilibrium cesium cells which convert 74% of the incident D^+ beam into D^- ions. The D^- beam must be extracted after leaving each cell. From this point, the negative ion beam must go through a multistage acceleration system which is essentially the same as if the beam had been one of positive ions. Clearly, the use of negative ions does not simplify the technological requirements of reaching high voltage. Once at high voltage, however, the D^- beam is passed through a neutralization cell consisting of D_2 gas and, as seen in Fig. 5-2, the conversion efficiency is ~70%. Importantly, since D^- is the only species emerging from the extraction system, one does not have the concerns as when half and third energy fast atoms are also injected into the plasma. This can help minimize the potential for charge exchange near the edge. This system could achieve an efficiency approaching 50% without direct conversion

which is much superior to the possibilities with positive ions at these energies. On the other hand, the current density in this conceptual design was on 0.015 A/cm^2 compared with the desireable range of 1-2 A/cm^2.

Direct conversion on the unneutralized portion of the ion beam, whether positive or negative ions, is a promising but very little developed method for improving overall beam system efficiency.[47,48] In Ref. 47, Moir describes a system in which the positive and negative ions emerging from a given cesium cell are separated by a bending magnet. The positive ions pass to a thermal convertor while the negative ions are accelerated and passed through a neutralizer. The unconverted D^- beam, now at high energy, is bent magnetically and transported to a direct convertor. Potentially such systems may give overall efficiencies of 80% at high energies but a very substantial development program is clearly required before such schemes are practical. A particular problem is handling the high power levels in the direct convertor.

Direct conversion can also be used to improve the efficiency of neutral beam systems based on positive ions. Moir et al.[47] have designed a 100 keV deuterium neutral beam system modeled after the LBL sources[33] in which the unneutralized D^+ part of the beam is directly converted at 80 kV with 69% efficiency. The molecular ion components are not converted. With direct conversion, the overall efficiency of this positive ion, 100 keV D° sources with fractional $D_2°$ and $D_3°$ components would be 71% efficient. Without the direct convertor but converting the unneutralized beam at 38% thermal efficiency gives a 60% overall efficiency. If the unneutralized beam is simply dumped, the overall efficiency drops to 50%. There is therefore considerable motivation to develop direct conversion for neutral beam systems but experimental work is today at a quite low level.

b. Neutral Beam Heating of Plasmas

Neutral beam injection for heating Tokamak plasmas has been extensively studied both experimentally and theoretically in the past several years. In particular, extensive experiments have been carried out on the Adiabatic Toroidal Compressor (ATC)[49,50] and on Ormak.[51,52] Recently, the central ion temperature on ORMAK has been doubled[20], from ~500 eV to ~1000 eV, with no apparent sign of anomolous behavior. On ATC,[50] ion temperature approaching 1500 eV and poloidal beta (β_θ) values exceeding 1 have been achieved. These results provide a strong experimental basis for the usefulness of neutral beam heating. Importantly, the experimental results are in general agreement with a quite detailed theory of neutral beam injection heating.[53,54] There does not appear to be any experimental deviation from the predictions of classical slowing down theory when the theory is properly corrected for particles lost from the machine because their orbits are unconfined.[54] In addition, Berk et al.[55,56] recently carried out a survey of possible microinstabilities which could effect the performance of two component tokamaks. This is particularly important because if such instabilities were to cause the beam to slow down faster than classically predicted, the plasma Q factor (fusion energy produced divided by input injected power) would drop. Their analysis showed that for typical beam-plasma parameters characteristic of next generation tokamaks, the system is stable to high frequency modes when a continuous, monoenergetic beam is injected parallel to the toroidal field, i.e., tangent to the magnetic axis. The general conditions correspond to values of Γ (beam pressure divided by background plasma pressure) less than about one.

Rosenbluth and Rutherford[57] have considered the excitation of shear Alfvén waves where $\omega \geq k_{\|}(r)\ v_A > k_{\|}(r)\ v_b$ within a particular minor radius due to spatially non-uniform beam injection. v_A is the Alfvén speed and v_b is the neutral injection beam velocity. The high energy beam ions can interact resonantly with waves by means of their ∇B drifts. The interaction is destabilizing when the diamagnetic drift frequency,

$$\omega_{*b} = -\ (m\ T_b/eBr)\ d\ \ln\ n_b/dr \quad ,$$

exceeds the shear Alfvén eigenmode frequency

$$\omega_A = k_{\|}(r)\ v_A + (nq - m + 1)\ v_A/q\ R \tag{20}$$

where m is the poloidal eigenvalue, n is the toroidal eigenvalue, and q is the safety factor.

For the tokamak fusion test reactor (TFTR)[58] with ~100 keV neutral beams, they predict a possible beam instability and anomolous flattening of the beam profile in the innermost 15 cm. For reactor conditions where the beam is effectively generated by α-particles at 3.5 MeV and $v_b \simeq v_A$, the inner 80 cm radius could be affected by the excitation of shear Alfvén waves. This connection between beam injection and Alfvén wave excitation is most intriguing and is bound to receive more attention in future work.

A potential problem for neutral beam injection in hot, reactor-like tokamaks is the beam-edge instability discussed by Girard et al.,[59] by

Conn et al.,[44] and by Hogan.[60] This problem is related to the effect of impurities on neutral beam penetration. For high energy injection (H° > 50 keV, D° > 100 keV), the primary ionization mechanism in the plasma is ion impact ionization. This cross section[61] is proportional to Z_{eff} which is defined as

$$Z_{eff} = \frac{\sum_j n_j Z_j^2}{n_e} \tag{21}$$

where the sum extends over all ionic species. As Z_{eff} increases, the neutral beam is more rapidly attenuated and penetration to the plasma center becomes more difficult. Furthermore, a beam attenuated more rapidly heats the edge preferentially and this is where the cold neutral gas population is highest. As a result, the effective energy of the charge exchange neutrals coming out of the plasma is increased. In turn, this causes an increase in the sputtering yield. The resulting increase in impurity content causes a further attenuation of the beam until little external heating reaches the center and the plasma cools. An example of the neutral beam penetration profile neglecting impurities and including them is shown in Fig. 5-3. Thus, impurities will affect the ability of neutral beams to penetrate plasmas and may have a detrimental effect on the overall energy balance if the beam edge instability is not controlled.

An important question is how high the energy of neutral beams must be to penetrate reactor grade tokamaks. This is particularly relevant when one recalls the discussion of the previous section on the technical difficulties of achieving high power, high energy, and high efficiency neutral beam sources. McAlees and Conn[37] considered this question for the UWMAK-I tokamak conceptual reactor.[46] This system has a circular plasma with a major radius of 13m and a plasma radius of 5m. It was found that even for relatively low density startup plasmas ($\bar{n} \sim 1.5 \times 10^{13}$ cm^{-3}), D° beam energies of 400-500 keV would be required to penetrate even with $Z_{eff} = 1$. For a similar system of plasma radius equal to 2m, 200 keV

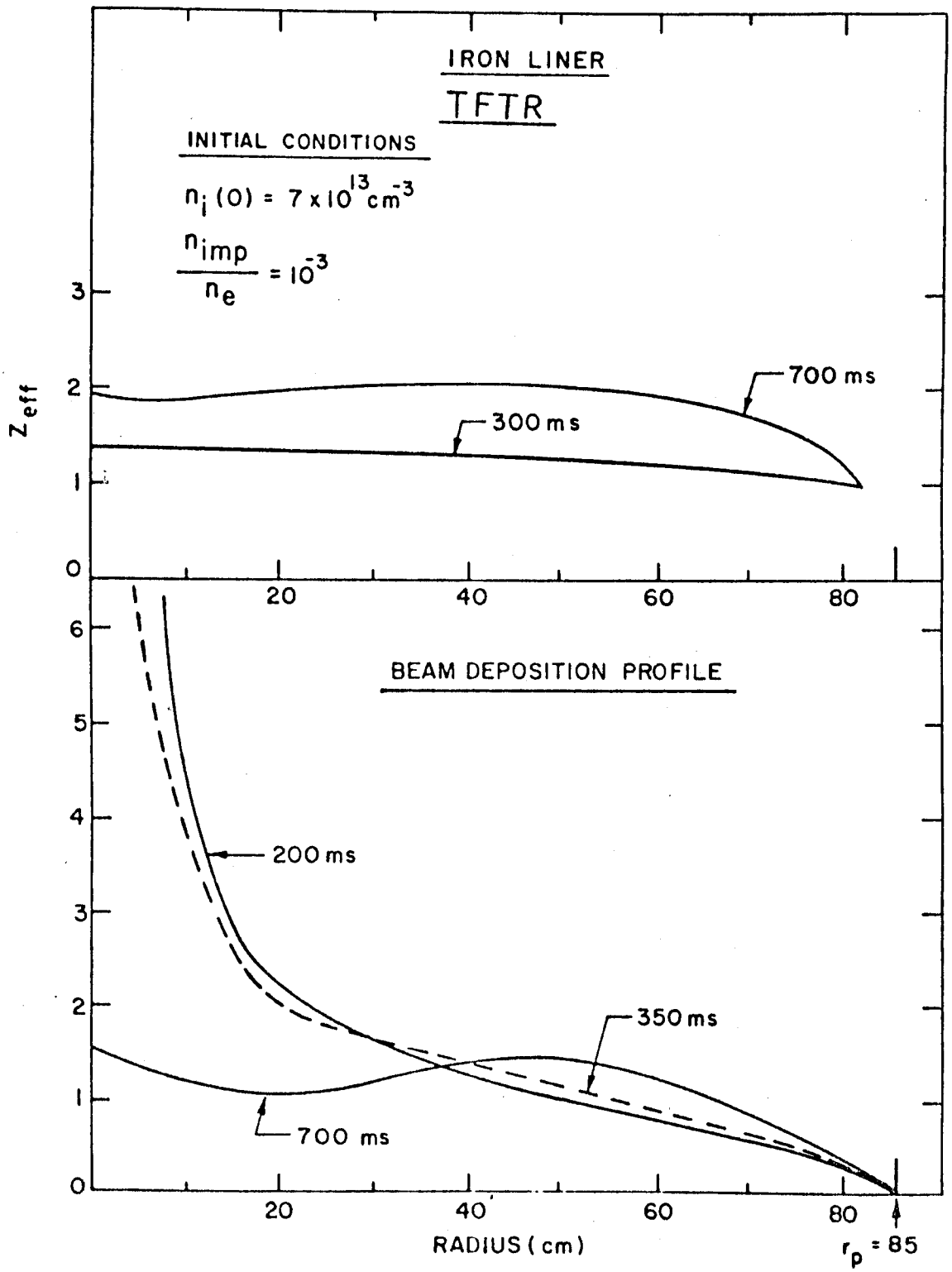

FIGURE 5-3

Z_{eff} and neutral beam energy deposition profile at various times in a two component tokamak, TFTR, with I_p = 2.5 MA and plasma radius, 85 cm.

D° is required. If the plasma density is higher (e.g. near $10^{14} cm^{-3}$) and Z_{eff} is greater than 1, even higher energy deuterium neutral beams would be required.

The UWMAK-III conceptual tokamak reactor is a noncircular system with a plasma height to width ratio of about 2. One of the advantages of noncircular devices should be the ability to reach higher values of total β for similar values of β_θ and stability factor, q. However, high density will mean that high energy neutral beams are required to penetrate. We have investigated this problem for UWMAK-III using both H° and D° beams.

The use of H° rather than D° may be very attractive for reactors since one requires only half the energy of H° to achieve the same beam penetration characteristics as with D°. The neutral beam efficiency for a D° beam will be about the same as that of an H° beam at half the energy. However, it should be simpler to design the lower voltage system. We will address the question of plasma buildup of H^+ shortly.

The geometry parameters of UWMAK-III relevant to beam injection calculations are listed in Table 5-1. The beam injection path is shown in Fig. 5-4. One sees that the beam is injected tangent to a circle of radius 6.9m. This is half way between the inner edge of the plasma and the plasma center and is close to optimum from a beam penetration viewpoint. For all calculations, the plasma temperature and density were assumed to be parabolic with respect to the minor radius.

The beam is attenuated along the injection chord according to

$$\frac{dB}{dS} = - \frac{n\langle\sigma v\rangle_{TOT}}{v_o} B \qquad (22)$$

Table 5-1

UWMAK-III Geometry Parameters Relevant for Beam Injection

Major Radius	8.1m
Plasma Radius	2.7m
Plasma Shape Factor ($\frac{\text{perimeter}}{\text{perimeter of inscribed circle}}$)	1.6
Cross Sectional Area/ Area of Inscribed Circle	2.17
Major Radius to Beam Path	6.9m

NEUTRAL BEAM INJECTION GEOMETRY

TOP VIEW OF TORUS

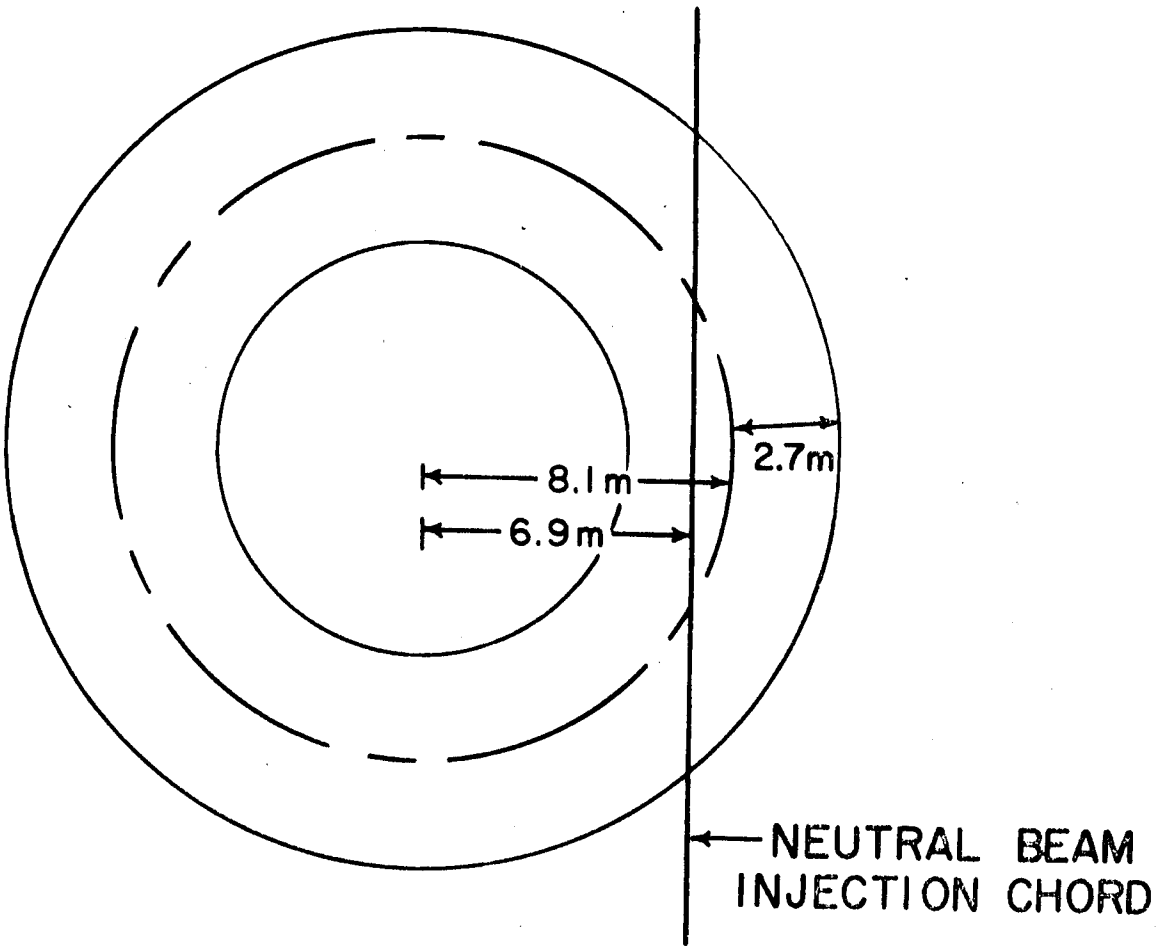

Figure 5-4 - Neutral beam injection geometry for the conceptual tokamak reactor, UWMAK-III

or

$$B(s) = B_o \exp\{- \frac{1}{v_o} \int_0^s n(s')[\langle\sigma v\rangle_{TOT}(s')]ds' \quad (23)$$

where B is the beam intensity, s is the distance along the injection chord, and n(s) is the plasma density at position s. v_o is the velocity of the injected neutrals and $\langle\sigma v\rangle_{TOT}$ is the total reaction parameter for the beam with the plasma. The beam is attenuated by three major processes; ion impact ionization; electron impact ionization; and charge exchange. These cross sections are shown in Fig. 5-5. For high energy beams injected into a plasma, the ion impact and charge exchange terms are simply

$$\langle\sigma v\rangle = v_o(\sigma_{cx}(v_o) + \sigma_i(v_o)) \quad (24)$$

where σ_{cx} and σ_i are the charge exchange and impact ionization cross sections at speed v_o. The electron impact ionization cross section $\langle\sigma v\rangle_e$ is independent of beam energy because of the large electron thermal velocity but of course depends on electron temperature, T_e.

For this noncircular tokamak problem, we have taken the central density to be $1.3 \times 10^{14} cm^{-3}$ and the central temperature to be 2.7 keV. This would be characteristic of startup conditions. We show in Fig. 5-6 the beam power deposited per unit volume of plasma as a function of normalized minor radius, r/a, for a 225 keV H° beam (case A) and a 325 keV H° beam (case B). This is equivalent to a 450 keV D° beam in case A and a 650 keV D° beam in case B. One can see that for case A, the profile is reasonably uniform across the plasma and peaks at the center. However, this can be misleading since what is important is the power deposited per plasma particle, i.e. the local power deposited per unit volume divided by the local plasma density. This is shown in Fig. 5-7 and one can see that

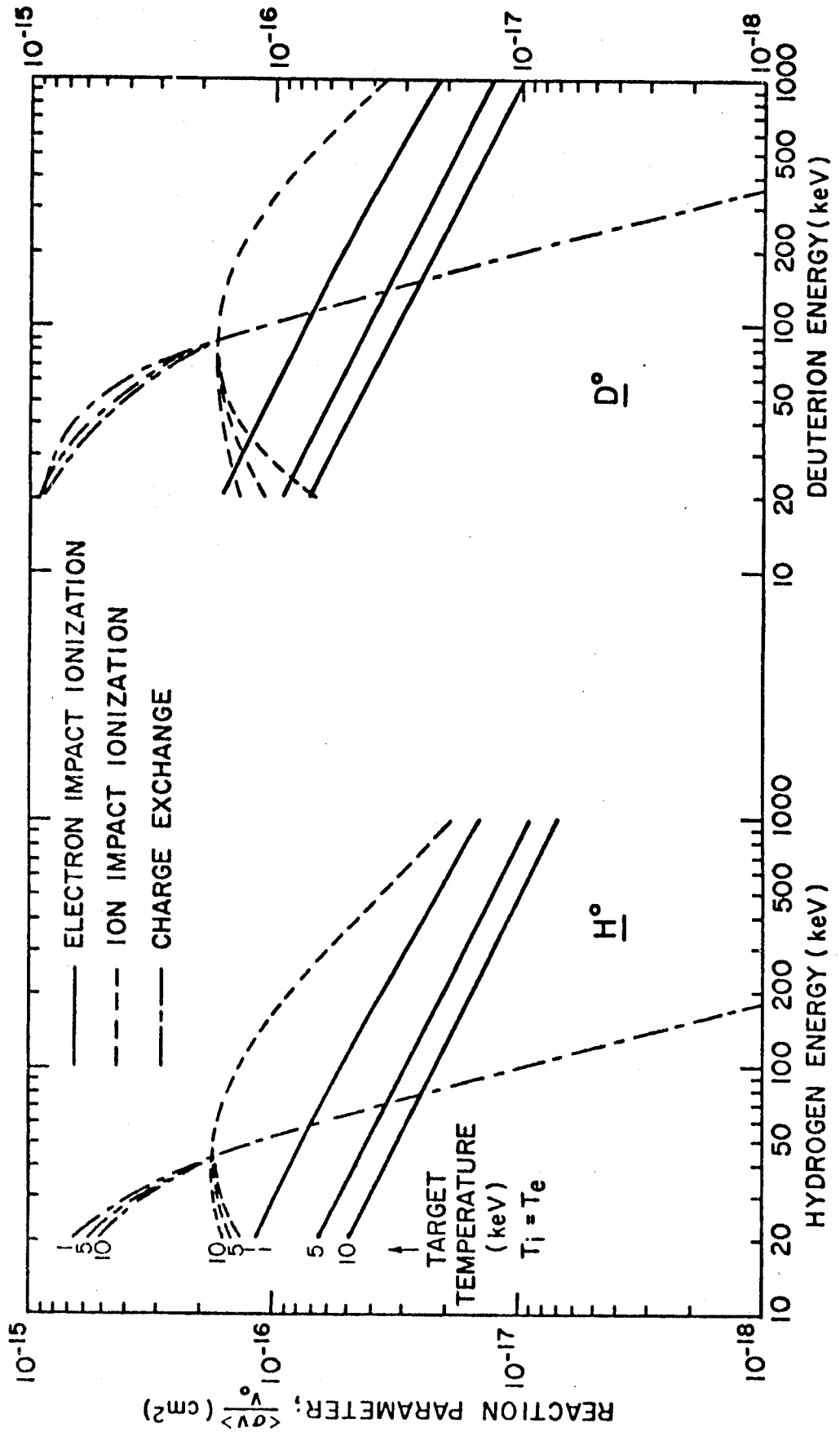

Figure 5-5 - Relevant cross sections for H° and D° beams incident on a target plasma. The target plasma is relevant only for low values of beam energy (<40 keV H°, <80 keV D°). In these cases, the plasma is assumed to be a 50-50 D-T mixture with $T_i = T_e$ and the cross sections are averaged over a Maxwellian distribution of target particles. Above 40 keV H° or 80 keV D°, the ion impact ionization and charge exchange reaction parameters essentially equal the microscopic cross sections.

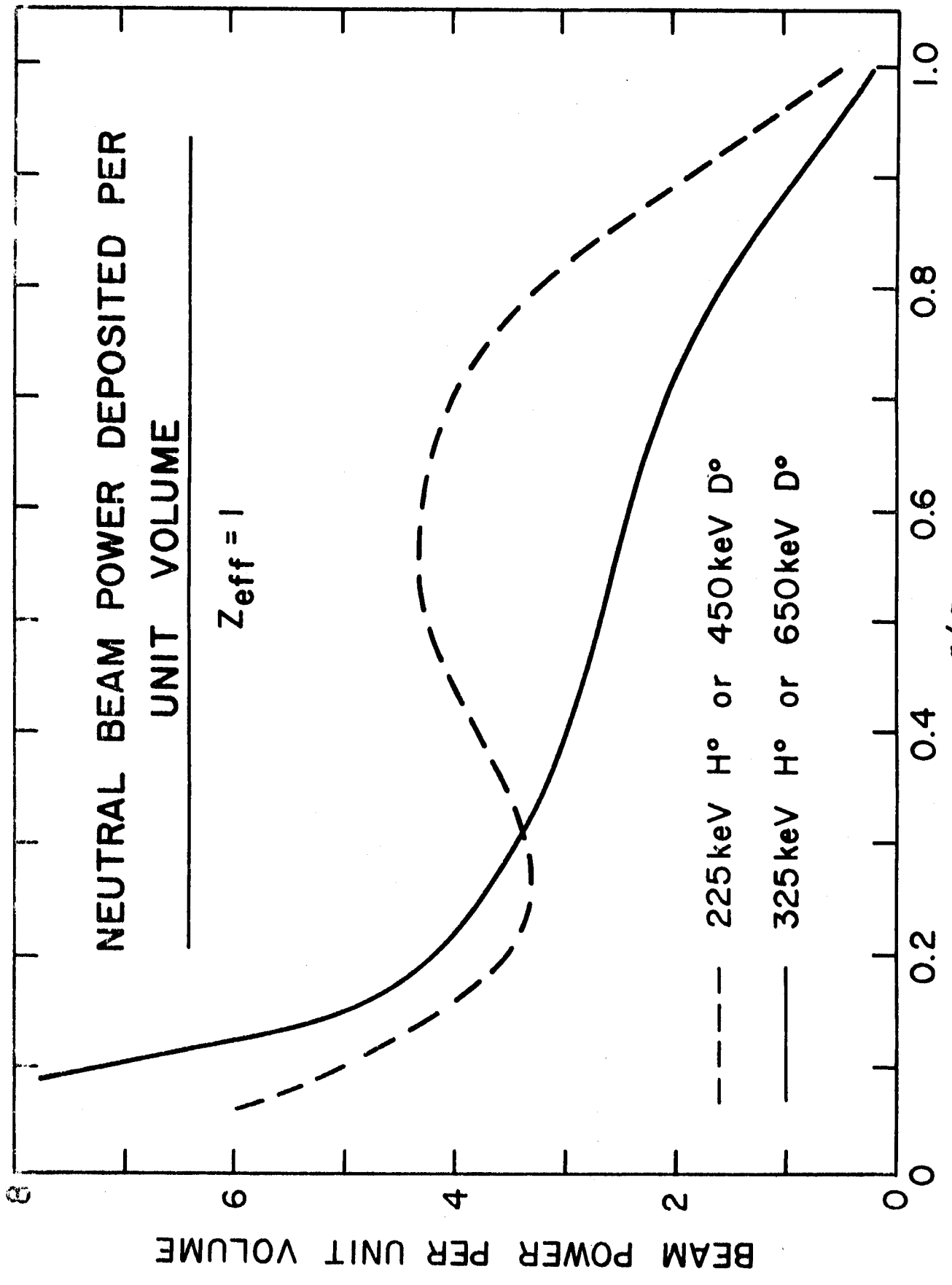

Figure 5-6 - Radial profile of beam deposition as a function of reduced radius for UWMAK-III. a is 2.7 m.

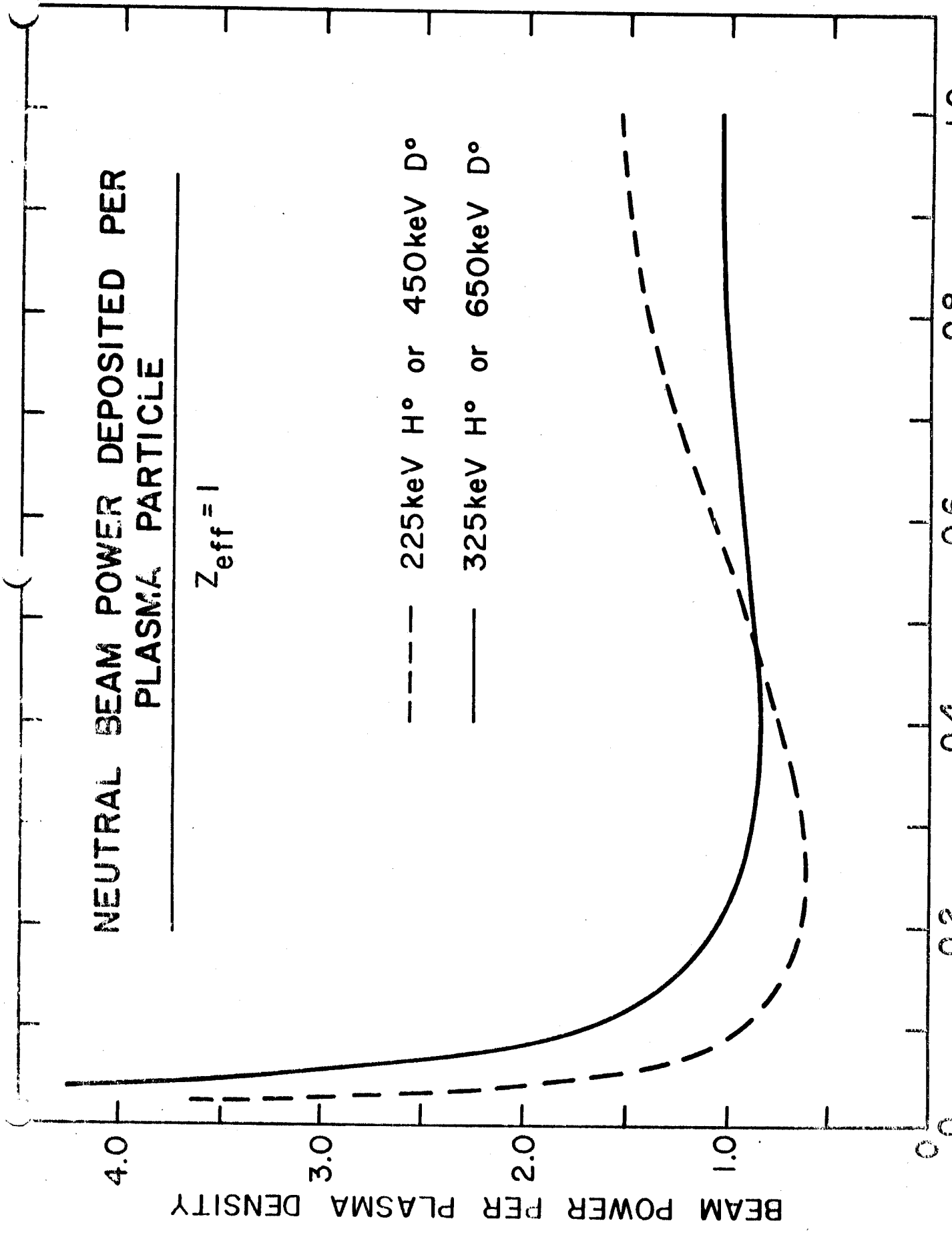

Figure 5-7 - Radial profile of beam deposition per unit volume divided by the plasma density profile for UWMAK-III.

even a 225 keV H° beam (450 keV D°) does not penetrate well and would lead to considerable edge heating.

Impurities have a considerable influence on the penetration characteristics of high energy beams since, as noted earlier, the ion impact ionization cross section is proportional to Z_{eff}. This effect is shown in Fig. 5-8 for a 225 keV H° beam or a 450 keV D° beam into UWMAK-III. The edge heating would be substantially increased while the central heating is correspondingly decreased.

These results show that for noncircular tokamak reactor size systems with average densities of ~6 x 10^{13} cm^{-3} or greater, hydrogen neutral beams of 200 keV or greater (or deuteron beams of 400 keV or greater) will be required to achieve the most desirable beam deposition profiles.

More near term devices will probably have similar values of plasma density but will be of smaller size. The beam energy requirements for penetration in these devices can approximately be determined by keeping constant the ratio of plasma half width to neutral beam mean free path. For this, we need an approximation to the total cross section for beam attenuation. This has been plotted by Sweetman[62] and a fit to that data valid to about 20% for H° energies in the range, 20 keV to 1 MeV (D° energies of 40 keV to 2 MeV) is

$$\frac{1}{\sigma_T} = 6 \times 10^{10} (W_o)^{.975} \ (cm^{-2}) \ \text{(for H°)} \tag{25}$$

$$\frac{1}{\sigma_T} = 3 \times 10^{10} (W_o)^{.975} \ (cm^{-2}) \ \text{(for D°)} \tag{26}$$

where W_o is the neutral atom energy in eV. The plasma density we have used has a parabolic distribution with a central density of 1.3 x 10^{14} cm^{-3}. Using the average density, 6.5 x 10^{13} cm^{-3}, the mean free path for a neutral is

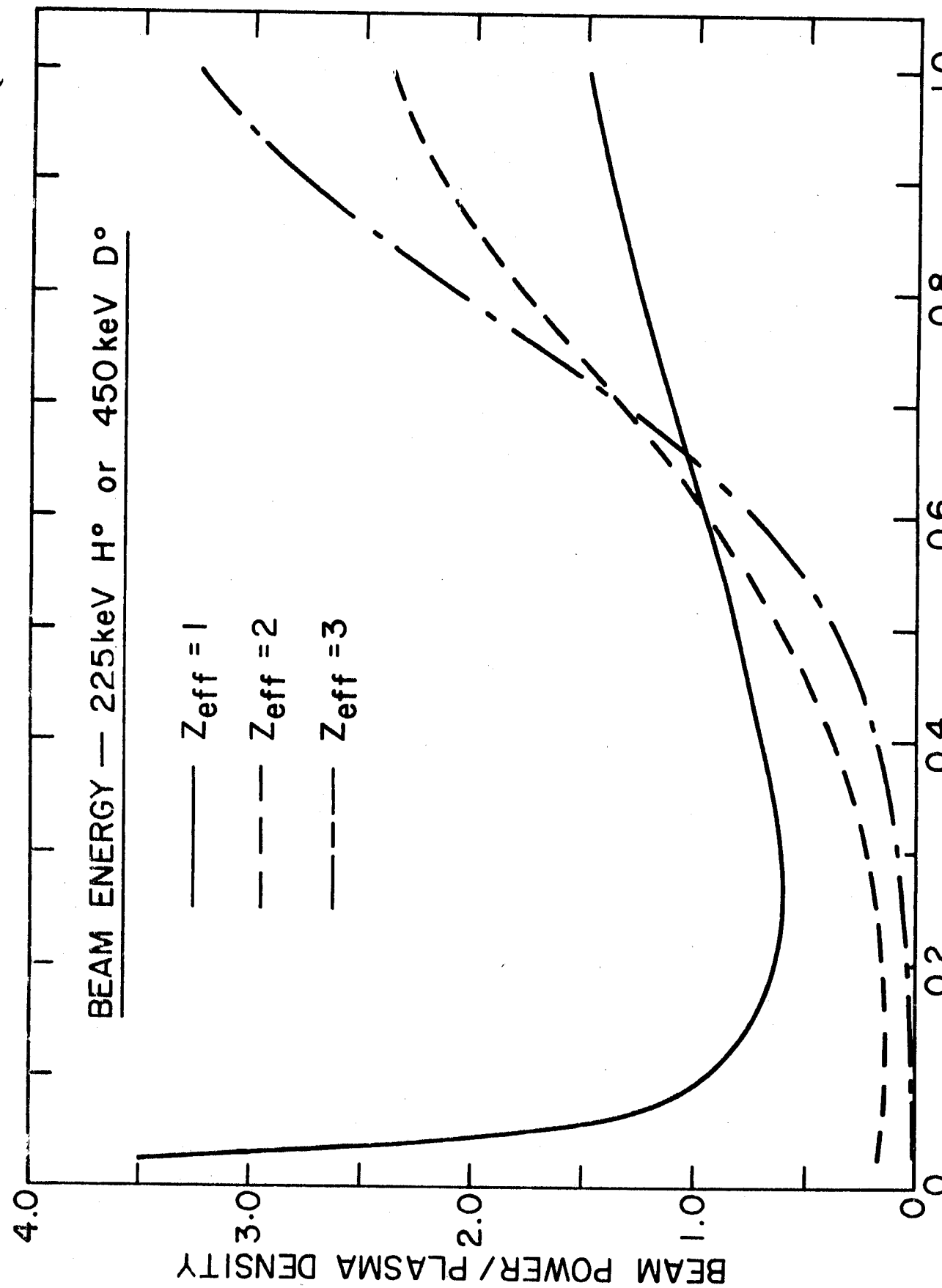

Figure 5-8 - Effect of impurities on the penetration characteristics of neutral beams injected into a reactor plasma such as UWMAK-III.

$$\lambda = 9.23 \times 10^{-4} \, (W_o)^{.975} \ . \ (cm) \qquad (27)$$

Thus, using a = 270 cm, a/λ is $2.93 \times 10^{5} \, (W_o)^{.975}$. (Note that when ion impact ionization is dominant, one can account for impurities by using $\lambda = 9.23 \times 10^{-4} \, (W_o)^{.975} / Z_{eff}$.)

Let us take a = 1m as typical of near term devices. The required neutral beam energy to achieve a beam deposition profile similar to that of the 225 keV H° (450 keV D°) beam in UWMAK-III, with $Z_{eff} = 1$, is then 80 keV H° (or 160 keV D°). Increasing Z_{eff} will have an effect similar to that shown in Figs. 5-3 and 5-8. Therefore, even in smaller, near term reactor systems, hydrogen neutral beams with energies of 80 keV or greater and deuteron beams of 160 keV or greater will be required to achieve adequate penetration. For two component tokamaks, which must have D° beams, the energy requirements for engineering test reactor or hybrid reactor applications will be at least 200 keV D°.[6] Also, these systems will most likely require neutral beam efficiencies of 50% or greater and can effectively use only the D° component (D_2° and D_3° are too low in energy). Thus, negative ion sources are most desirable. Yet, as discussed in the previous section, such sources require the greatest amount of development before they can be practical systems.

As we have described, the use of H° means that only half the voltage is required to achieve the same beam penetration characteristics as with a D° beam. This can significantly lower the number of accelerating stages required in the neutral beam system (whether positive or negative ions are used,) thus easing the technical requirements. A problem can be the buildup of H° in the D-T plasma. This would in turn reduce the effective fuel density and the fusion power generated during heatup to ignition.

The hydrogen density buildup and decay satisfies the global equation

$$\frac{dN_H}{dt} = I_H - \frac{N_H}{\tau_p} \qquad (28)$$

where N_H is the number of hydrogen ions, I_H is the hydrogen beam current in H° atoms per second, and τ_p is the particle confinement time. During injection, N_H is given by

$$N_H(t) = I_H \tau_p(1 - e^{-t/\tau_p}). \quad 0 \leq t \leq t_1 \tag{29}$$

Once the beam is turned off, say at t_1, the particle number decays as

$$N_H(t) = N_H(t_1)e^{-t/\tau_p}. \quad t \geq t_1 \tag{30}$$

The important point to recall is that beams injected at high energy per particle do not inject many particles by comparison to the total number of background particles. As such, the hydrogen density will not be large. To show this, we consider as an example the heating of UWMAK-III. We use parameters similar to those studied for RF heating. There are two cases, injection of 40 MW for 12 seconds (case 1) and the injection of 200 MW for 1.34 seconds (case 2). Let us assume that we inject H° beams at 225 keV.

In case 1, 40 MW corresponds to an H° injection rate of 1.1×10^{21} H°/sec. During the injection phase, let us take τ_p as 1 sec. Then after 12 sec, the number of hydrogen atoms in the plasma is essentially 1.1×10^{21}. If τ_p is 10 sec (which is quite optimistic), then N_H (12 sec) $\simeq 7.7 \times 10^{21}$ (H° atoms). These values must be compared to the steady state number of D + T ions. For an average density of $6.5 \times 10^{13} cm^{-3}$ and a plasma volume of $2.37 \times 10^{9} cm^{3}$. $N_{D+T} = 1.54 \times 10^{23}$ (D+T) ions. Thus, for $\tau_p = 1$ sec, $\frac{N_H}{N_{D+T}}$ is just 0.007. For $\tau_p = 10$ sec, it is only 0.05. In neither case does the hydrogen density become more than 10% of the steady state D+T fuel density. For case 2, (200 MW injection for 1.34 sec.), the maximum hydrogen concentration relative to the D+T fuel concentration is less than 1% for $\tau_p = 1$ sec and about 3% for $\tau_p = 10$ sec. Thus, the injection of lower energy neutral hydrogen can significantly ease the voltage requirements while not having much effect on the background plasma density.

A final characteristic of neutral beam heating is the fraction of beam energy going directly to the plasma ions. An analytical expression for the fraction of test particle energy going to all ion species (which rapidly thermalized together) is[63]

$$f_i = \frac{1}{3}\frac{E_c}{W_o}\left\{\ell n\left[\frac{E_c - (E_c W_o)^{1/2} + W_o}{E_c + 2(E_c W_o)^{1/2} + W_o}\right]\right.$$

$$\left. - 2\sqrt{3}\tan^{-1}\left[\frac{2 W_o^{1/2} - E_c^{1/2}}{\sqrt{3}\, E_c^{1/2}} + \frac{\sqrt{3}\,\pi}{3}\right]\right\} . \qquad (31)$$

Here, W_o is the injection energy and E_c is the energy at which the rate of energy loss to all ion species is equal to the rate of energy loss to the electrons. It is given by

$$E_c = 14.8\, A_T\, T_e\left[\frac{1}{n_e \ell n\Lambda_e}\sum_j \frac{n_j Z_j^2 \ell n\Lambda_j}{A_j}\right] \qquad (32)$$

where A_T is the atomic mass of the injected species and the sum j extends over all ionic species. A plot of f_i as a function of the electron temperature, T_e, is shown in Fig. 5-9 for H^o and D^o beams at 100 keV and 500 keV. As the energy of injection increases, f_i decreases so that, e.g., for $T_e < 10$ keV and $W_o = 500$ keV, less than 50% of the energy goes directly to the ions for D^o and less than 25% for H^o. This is relevant in cases where the energy confinement time of the electrons is anomolously short, particularly by comparison with the electron-ion rethermalization time, while the ion confinement time is acceptably long. This can be the case when impurities cause excessive energy loss from electrons.[63] However, the cause need not be specified.[65] It has been found[63,65] that

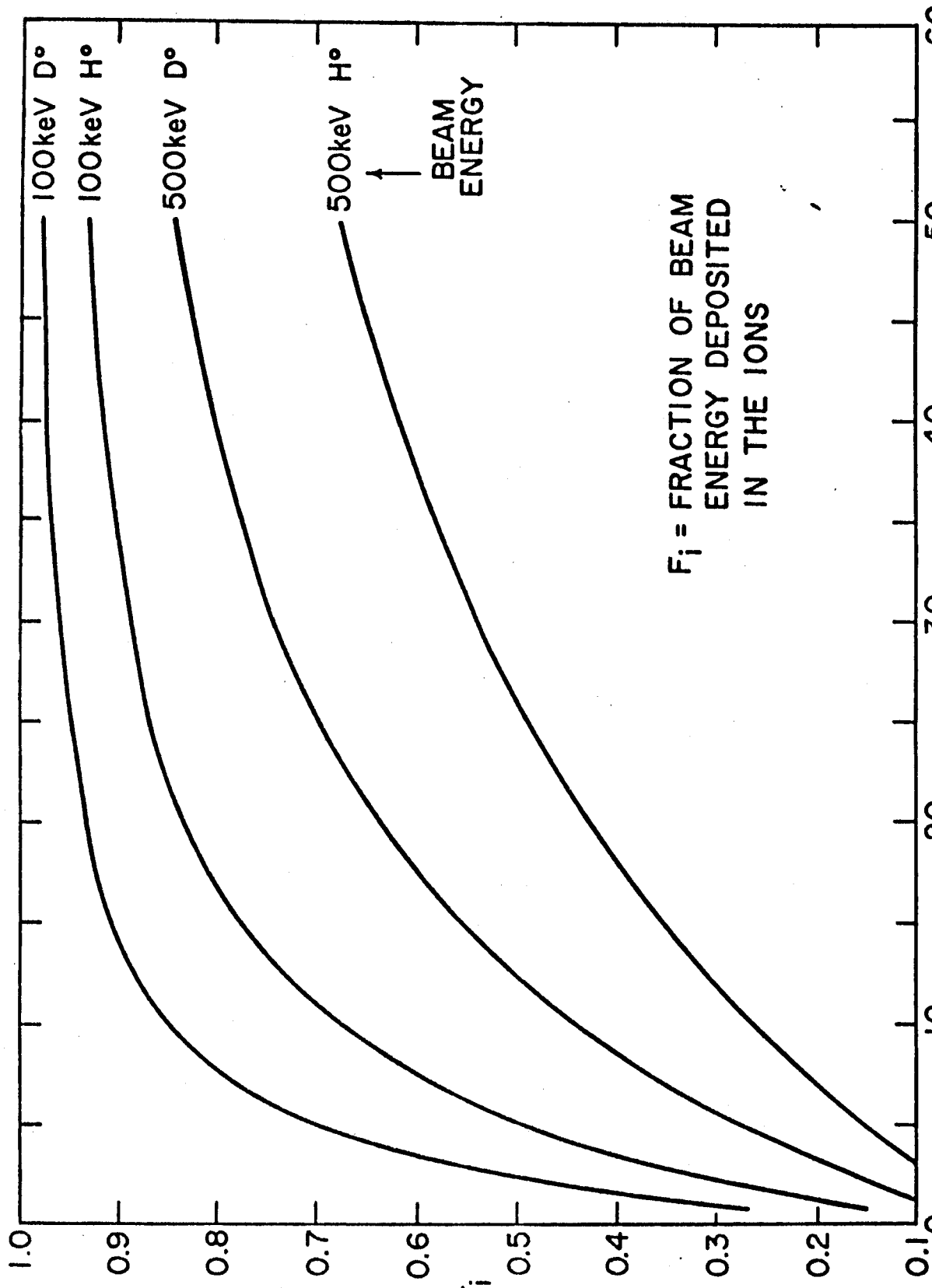

Figure 5-9 - Fraction of neutral beam energy deposited directly into the ions as a function of electron temperature, beam energy, and the mass of the neutral.

high overall plasma energy amplification factors can nevertheless be achieved but it is necessary to keep the ions hot by direct supply of energy. As such, the low values of f_i at low T_e are detrimental. If RF heating can supply energy directly to the ions, it will have a significant advantage over beams in such an application.

6. Qualitative Comparison of the Present Status and Reactor Potential of RF and Neutral Beam Heating

In this section, we present our opinions regarding the present status and future potential of RF and neutral beam injection heating. These opinions are based on both the work reported in this paper and on our previous efforts related to the study of tokamak reactor problems.

RF sources for heating at frequencies of 60 MHz or less are presently available at power levels close to those which will be required for reactors (5-10 MW per module.) Development will be required to achieve pulse widths in the 1-10 second range but the efficiency of the sources will be greater than 50%. Therefore, source development for RF heating at $\lesssim$ 60 MHz is required but the extrapolation is moderate and reasonable. By contrast, neutral beam sources will require major further development to meet the requirements of reactor systems (10 MW per module at beam energies greater than or equal to 200 keV for 1-10 seconds with at least 50% efficiencies). Present day sources utilize positive ions and use of single stage acceleration. To achieve injection energies exceeding 200 keV, multistage acceleration is required and to achieve overall efficiencies exceeding 50%, negative ion sources will be required. Both these areas represent substantial technological advancements. We would argue therefore that RF sources are presently closer to the desired operating goals than are neutral beam sources.

On the other hand, the present status of neutral beam heating experiments and their correlation with theory are both very good. Neutral beam heating experiments on ATC,[66] ORMAK,[67] and TFR[68] all show substantial plasma heating and the results are in good agreement with a highly developed theory.[53,54]

Further, in terms of applications to two component tokamaks, neutral beam injection is preferred in that it will potentially yield at least twoce as

large a plasma energy amplification factor, Q, as in an RF driven device.[23]

By contrast, few high power wave experiments have been conducted in tokamak plasmas. The ST fast magnetosonic wave heating experiment[3] exhibited wave generation efficiencies of up to 90% and good agreement with theoretically predicted toroidal eigenmodes. At $\omega = 2\omega_{ci}$ it was necessary to operate the device at 25kA discharge current and 16 kG toroidal field in order to excite the waves from the 25 MHz generator that was available. However, high power levels caused a significant influx of neutral particles. This observation is explained by the heating of ions with high transverse energy which are on banana orbits and which strike the limiter or walls. At higher discharge currents contemplated in larger devices, the corresponding poloidal magnetic field will provide much better confinement for ions heated on banana orbits by fast waves. One would have to classify the success of the high power fast wave experiment as moderate. Thus what is called for is a definitive fast wave heating experiment for a larger tokamak device.

In reactor applications, two potential advantages of low frequency RF heating may be the ability to control the spatial distribution of the heating and the ability to control the fraction of energy deposited in the ionic species and the electrons. To a lesser extent, this is also possible with neutral beams. However, beam energy is the only controlling factor and while a high beam energy improves penetration, it also leads to a increase in the fraction of beam energy deposited with the electrons.

For neutral beams, the design of the injector ports is relatively straight forward compared with the problems of designing a launching structure for RF heating. The penetration and heating of waves is determined by the toroidal and poloidal k-space spectrum of the launching structure. Thus the structure

has to be designed to excite the most desireable heating modes. Further, if dielectrics are used appropriate shields will have to be designed to protect the material from the reactor particle and neutron fluxes. More information on RF breakdown in a dilute plasma environment is required.

On the other hand, shielding the neutral beam injector from neutron bombardment may be a difficult problem, particularly if the source design does not readily permit bending of the ion beam prior to its entry into the neutralization cell. This is the case at the present time. RF sources can more readily be protected from direct neutron bombardment by designing a coupled coax-waveguide feed system as described in the UWMAK-III reactor study.[29] By using a vacuum filled guide, as the last section of wave feed, a 90° wave guide to coax transition can be used to isolate the wave source from the reactor neutron flux. As shown in Fig. 3-3, a neutron shield can be built around the end of the guide.

In the physics area, the problems with neutral beam injection do not appear to be major, as illustrated by the present good agreement between theory and experiment. There may be problems with beam penetration and the beam-edge instability if impurity influx is a major problem. By contrast relatively little work has been done on the effect of impurities on RF heating.[69] Both heating schemes could benefit from divertor impurity control. Further theoretical work on RF heating is called for to determine the velocity distributions of heated particles and to analyse whether these distributions can drive microinstabilities.

Overall, we would conclude that the present status of experiment and theory for neutral beam injection heating is better than for low frequency RF heating. Extrapolating to reactors, neutral beams appear to be more advantageous for two component tokamaks which may be used in conjunction with fusion-fission systems. On the other hand, RF offers some distinct potential advantages for heating reactor plasmas to ignition conditions. Further, while the physics base for neutral injection is more firm at the present time, the technological extrapolations required for reactor applications are less for RF heating. As such, we would conclude that a vigorous program in source technology is required for further development of neutral beams. In fact, a program of this type now exists. For RF, fast magnetosonic and lower hybrid heating experiments are needed to clearly establish the physics base in this area. What is needed here is a vigorous program to provide definitive tests of the viability of high power RF heating. Both approaches offer advantages that depend on the final application. It would be premature to chose between these heating methods without further experimental and theoretical investigations in both areas.

Table 6-1

		RF	Neutral Beams
1.	Capability of Present Sources	4 MW (10 ms) @ 25 MHz	250 kW (200 ms) @ 40 keV
2.	Anticipated Near Term Source Capability	10 MW (300 ms) @ 55 MHz	1 MW (500 ms) @ 80-120 keV
3.	Present Status from Plasma Physics Viewpoint		
	a. Theory	good-moderate	very good-no serious instabilities predicted
	b. Experiment	moderate-fair	very good
4.	Requirements for Tokamak Reactor Systems		
	a. Sources	100 MW (1-10s)	100 MW (1-10s)@ >200 keV
	b. Source Efficiency ($P_{out}/P_{D.C.}$)	>50%	>50%
5.	Potential Advantages for Reactor Applications	a. Moderate Source Development to achieve overall efficiencies >50% at desired frequencies (1-60 MHz) and power levels per module (10 MW) b. Low Γ = $\frac{\text{wave energy density}}{\text{plasma energy density}}$ c. Potential for precise resolution of the spatial distribution of heating and of energy deposited in ionic species. d. Potential to bend wave delivery system so as to protect sources from neutron heating and minimize neutron leakage.	a. Heating should be stable b. Beam ports are simple c. Good agreement between present theory and experiment d. High Q in two component plasma applications

Table 6-1 (con't)

		RF	Neutral Beams
6.	Potential Problems and Questions for Reactor Applications		
	a. Technological Design	a. Launching structure design waveguides vs. coils	a. Protection of source from neutron bombardment
		b. Arcing at high powers	b. Efficiency of the source when beam energy >150 keV
		c. If dielectrics are required, how will they behave in reactor environment?	c. Technological advancements for high voltage sources-operation of multistaged injectors.
	b. Physics	a. Confinement of heated plasmas	a. Beam penetration - especially if $Z_{eff} > 2$ or there is high density as in noncircular devices.
		b. Production of microinstabilities	b. Beam-edge instability caused by impurities
		c. Effects of impurities on heating	c. Alfvén wave excitation and effect on beam profile
		d. Nonlinear wave effects	

ACKNOWLEDGEMENT

This work was supported in part by EPRI. We would also like to acknowledge the help of Dr. Jay Kesner and Wayne Houlberg with the calculations.

References

1. Hooke, W. M., Hosea, J. L. "Wave Generation and Heating Near the Ion Cyclotron Frequency in the ST Tokamak", Vth European Conference on Controlled Fusion and Plasma Physics (Grenoble, 1972).

2. Hosea, J. L., Hooke, W. M., "Ion Cyclotron and Fast Hydromagnetic Wave Generation in the ST Tokamak", Phys. Rev. Lett. 31, 150 (1973).

3. Adam, J. Chance, M., Eubank, H., Getty, W., Hinnov, E., Hooke, W., Hosea, J., Hones, F., Perkins, F., Sinclair, R., Sperling, J., Takahasi, H. "Wave Generation and Heating in the ST Tokamak at the Fundamental and Harmonic Ion Cyclotron Frequencies", 5th International Conf. on Plasma Physics and Controlled Fusion Research (Tokyo 1974) IAEA-CN-33/G1-2.

4. Hosea, J. L. "Fast and Slow Ion Cyclotron Wave Generation and Heating in the ST Tokamak," Princeton University, Plasma Physics Laboratory MATT-1129.

5. Yamato, H., Iihoshi, A., Rothman, M. A., Sinclair, R. M., Yoshikawa, S., Phys. Fluids 10, 756 (1967).

6. Rothman, M. A., Sinclair, R. M., Brown, I. G., Hosea, J. L. "Ion Cyclotron Heating in the Model C Stellerator," Phys. Fluids 12, 2211 (1967).

7. Adam, J. and Samain, A. "Chauffage par Absorption Cyclotronique." Rapport du Groupe d'etude du Chauffage d'un Plasma, Confine dans une Configuration Magnetique du Type Tokamak. Report EUR-CEA-FC-579.

8. Ivanov, N. V., Brown, I. A., Los', E. V., Sov. Phys. JETP Lett. 14 138 (1971) also Atomnaya Energiya 32, 389 (1972).

9. Perkins, F. W., "Hydromagnetic Wave Heating of Tokamak Plasmas," Symposium on Plasma Heating and Injection, (Varenna, 1972).

10. Hooke, W. M., Perkins, F. W., Stix, T. H., Takahashi, H., Dietz, A., Lawson, J. W., Christie, R., Kloiber, F., Newman, W., Siva, A., "Proposal for the High-Power ICRH Wave-Heating Facility for the PLT Tokamak."

11. Stix, T. H., Phys. Rev. Lett. 15, 878 (1965).

12. Briggs, R. J., Parker, R. R., Phys. Rev. Lett. 29, 852 (1972).

13. Golant, V. E., Zh. Tekh. Fiz. 41, 2492 (1971) [Sov. Phys. Tech. Phys. 16, 1980 (1972)].

14. Troyon, F., Perkins, F. W., Proceedings 2nd Topical Conference on RF Plasma Heating, Texas Tech. Univ., Lubbock, Texas (1974).

15. Bers, Abraham, "Ion Heating in Tokamaks by Wave Penetration and Parametric Downconversion of RF Power" in Proceedings of the U.S. - Australian Workshop on Plasma Waves, Paper COO-3070-108 (1975).

16. Brambilla, M., in Proceedings of a Symposium on Plasma Heating in Toroidal Devices, Varenna, Italy (1974).

17. Bernabei S., Heald, M. A., Hooke, W. M., Paoloni, F. J., "Penetration of Slow Waves into a Dense Plasma Using a Phased Wave-Guide Array," Phys. Rev. Lett. 34, 866 (1975).

18. Hooke, W. M., Bull. Amer. Phys. Soc., 20, 1313 (1975).

19. Richards, B., Parker, R. R., Bull. Amer. Phys. Soc., 20, 1313 (1975).

20. Hasegawa, Akira, Chen, Lui, "Kinetic Process of Plasma Heating Due to Alfvén Wave Excitation," Phys. Rev. Lett. 35, 370 (1975).

21. Messiaen, A. M., Vandenplas, P. C., "Radio-Frequency Heating of Large Thermonuclear Tori," Fifth Conference on Plasma Physics and Controlled Nuclear Fusion Research (Tokyo, 1974) Paper IAEA-CN-33/C4-2.

22. Weynants, R. R., "Ion Heating at Twice the Ion Cyclotron Frequency in Reactor Oriented Machines", Phys. Rev. Letters 33, 78 (1974).

23. Stix, T. H., "Fast-Wave Heating of a Two-Component Plasma", Princeton University, Plasma Physics Laboratory MATT-1113.

24. Stix, T. H., The Theory of Plasma Waves, McGraw-Hill, New York 1962.

25. Swanson, D. G. and Ngan, Y. C., "Warm Plasma Effects on Fast Alfven Wave Cavity Resonances." Phys. Rev. Lett. 35, 517 (1975).

26. Scharer, J. E., May, T. K., Blackfield, D. T., McVey, B. D., "Fast Magnetosonic Wave Heating at the Second Ion Cyclotron Harmonic in Tokamak Plasmas," Proc. Seventh European Conference on Controlled Fusion and Plasma Physics, p. 145, Lausanne, September, 1975.

27. Mau, T. K., McVey, B. D., Scharer, J. E., Bull. Amer. Phys. Soc. 20, 1242 (1975).

28. Badger, B., et al. "UWMAK-II, A Conceptual Tokamak Reactor Design" Nucl. Eng. Dept. Report UWFDM-112 (University of Wisconsin, 1975).

29. Badger, B., et al., "UWMAK-III, A High Performance, Noncircular Tokamak Power Reactor Design" Nucl. Eng. Dept. Report UWFDM-150 (University of Wisconsin, 1975).

30. Weynants, R. R., "A High-Temperature, High Density Reduction of Harmonic Ion-Cyclotron Heating Efficiency", Symposium on Plasma Heating in Toroidal Devices, (Varenna, September 1974).

31. Cato, J. E., Kristiansen, M., and Hagler, M. O., "Some Engineering Problems of Low-Frequency Heating of Fusion Reactors," Nuclear Fusion 12, 345-352 (1972).

32. Cohn, Seymour B., "Properties of Ridged Wave Guide," Proc. I.R.E., 35, 783-788 (1974).

33. Stirling, W. L., et al. "Intense Ion Beam Production Below 40 keV," Proc. 2nd Int'l Conf. on Ion Sources, (IAEA, Vienna, 1972). p. 278.

34. Cooper, W. S., Beckner, K. H., Pyle, R. V., ibid. p. 264.

35. Stewart, L. D., et al. "Tokamak Neutral Beam Heating Technology," in Proc. First Topical Meeting on the Technology of Controlled Nuclear Fusion (CONF-740402-P1, USAEC, 1974) Vol. 1, p. 365.

36. Hamilton, G. W., Dexter, W. L., and Smith, B. H., "A Design of a Neutral Injection System for the FERF," ibid., p. 376.

37. McAlees, D. G., Conn, R. W., Nuclear Fusion 14 (1974) 419.

38. Conn, R. W., Jassby, D. L., "A Tokamak Engineering Test Reactor," Princeton Plasma Physics Lab. Report MATT-1155 (Aug. 1975) and Nucl. Eng. Dept. Report UWFDM-119 (March 1975; Univ. of Wisconsin).

39. Jassby, D. L., Nuclear Fusion 15 (1975) 453.

40. Kelley, G. G., IEEE Trans. on Nucl. Sci. 14 (1967) 29.

41. Sweetman, D. R., "Intense Ion Beam Production Below 40 keV," Proc. 2nd Int'l Conf. on Ion Sources, (IAEA, Vienna, 1972) p. 271.

42. Thompson, E., in Proc. 2nd Symp. on Ion Sources and Formation of Ion Beams (Berkeley, Ca., 1974) papers II-3, II-7.

43. Beckner, K. H., Pyle, P. V., Stearns, J. W., in Proc. First Topical Meeting on the Technology of Controlled Nuclear Fusion (CONF-740402-P1, USAEC, 1974) Vol. 1, p. 392.

44. Conn, R. W., Khelladi, M., Kesner, J., "Impurity Effects on Plasma Performance on Two Component Tokamaks," Nucl. Eng. Dept. Report UWFDM-136 (Oct. 1975, Univ. of Wisconsin).

45. Schlachter, A. S. et al., Phys. Rev. 177, 184 (1969).

46. Badger, B. et al., "UWMAK-I, A Wisconsin Toroidal Fusion Reactor Design," Nucl. Eng. Dept. Report UWFDM-68 (Univ. of Wisconsin, Nov. 1973).

47. Moir, R., in Proc. First Topical Meeting on the Technology of Controlled Nuclear Fusion (CONF-740402-P1, USAEC, 1974) Vol. 1, p. 432.

48. Moir, R. W. et al., "Progress on the Conceptual Design of a Mirror Hybrid Fusion-Fission Reactor," Lawrence Livermore Lab. Report UCRL-51797 (June 1975).

49. Bol, K. et al., Phys. Rev. Letts. 32 (1973) 661.

50. Hubank, H. P. et al., Bull. Am. Phys. Soc. 20 (1975) 1346.

51. Berry, L. A. et al. "Plasma Confinement in the ORMAK Device," in Plasma Physics and Controlled Nuclear Fusion Research 1974 (IAEA, Vienna, 1975) Vol. I, p. 113.

52. Berry, L. A. Bull. Am. Phys. Soc. 20 (1975) 1332.

53. Rome, J. A., Callen, J. D., Clarke, J. F., Nuclear Fusion 14 (1974) 141.

54. Callen, J. D., in Plasma Physics and Controlled Nuclear Fusion Research 1974 (IAEA, Vienna, 1975) Vol. I, p. 645, and J. D. Callen Bull. Amer. Phys. Soc. 20 (1975) 1331.

55. Berk, H. et al., in Plasma Physics and Controlled Nuclear Fusion Research 1974 (IAEA, Vienna, 1975) Vol. III, p. 569.

56. Berk, H., et al. Nuclear Fusion 15 (1975) 819.

57. Rosenbluth, M. N., Rutherford, P. H., "Excitation of Alfvén Waves by High-Energy Ions in a Tokamak," Phys. Rev. Lett. 34, 1428 (1975).

58. Two Component Torus, Joint Conceptual Design Study (Princeton Plasma Physics Laboratory and Westinghouse Electric Corp., June 1974) Vols. I, II, and III.

59. Girard, J. P., Marty, D. A., Moriette, P., in Plasma Physics and Controlled Nuclear Fusion Research 1974 (IAEA, Vienna, 1975) Vol. I, p. 681.

60. Hogan, J. Bull. Amer. Phys. Soc. 20 (1975) 1228.

61. McDaniel, E. W., Collision Phenomena in Ionized Gases (John Wiley and Sons, New York, 1964.)

62. Sweetman, D. R., Nuclear Fusion 13 (1973) 157.

63. Conn, R. W., Kesner, J., Nuclear Fusion 15 (1975) 775.

64. Stix, T., Plasma Physics 14 (1972) 367.

65. Dawson, J. M., Lin, A. T., "Some New Ideas on Wet Wood Burners," Plasma Physics Group Report PPG-218 (UCLA, April 1975).

66. Eubank, H. P., Bol, K., Ellis, R. A., Goldston, R. J., Nagashima, T., Bull. Amer. Phys. Soc. 20, 1346 (1975).
Goldston, R. J., Eubank, H. P., Bull. Amer. Phys. Soc. 20, 1346 (1975).

67. Berry, L. A., Bull. Amer. Phys. Soc. 20, 1332 (1975).

68. Dei Cas, R., Bull. Amer. Phys. Soc. 20 , 1332 (1975).

69. Takahashi, H., Bull. Amer. Phys. Soc. 19, 959 (1974).